A Study on
Wide-Area Controller Design and Effect of Delays in Power Systems

Thesis submitted to
National Institute of Technology, Rourkela
For award of the degree

of

Master of Technology
in
Control and Automation

by

Abhilash Patel

DEPARTMENT OF ELECTRICAL ENGINEERING
NATIONAL INSTITUTE OF TECHNOLOGY,ROURKELA

MAY 2015

A Study on
Wide-Area Controller Design and Effect of Delays in Power Systems

Thesis submitted to
National Institute of Technology, Rourkela
For award of the degree

of

Master of Technology
in
Control and Automation

by

Abhilash Patel

Under the guidance of

Prof. Sandip Ghosh

DEPARTMENT OF ELECTRICAL ENGINEERING
NATIONAL INSTITUTE OF TECHNOLOGY,ROURKELA

MAY 2015

Dedicated to

Bapa, Maa and Dada

DEPARTMENT OF ELECTRICAL ENGINEERING
NATIONAL INSTITUTE OF TECHNOLOGY, ROURKELA

CERTIFICATE

This is to certify that the thesis entitled **A Study on Wide-Area Controller Design and Effect of Delays in Power Systems**, submitted by **Abhilash Patel** to National Institute of Technology, Rourkela, is a record of bonafide research work under my supervision and I consider it worthy of consideration for award of the degree of **Master of Technology** in **Electrical Engineering** with specialization in **Control and Automation** from the institute.

The embodiment of this thesis is not submitted in any other university and/or institute for the award of any degree or diploma to the best of our knowledge and belief.

Prof. Sandip Ghosh
(Supervisor)

DECLARATION

I certify that

a. The work contained in this thesis is original and has been done by me under the general supervision of my supervisors.

b. The work has not been submitted to any other Institute for any degree or diploma.

c. I have followed the guidelines provided by the Institute in writing the thesis.

d. I have conformed to the norms and guidelines given in the Ethical Code of Conduct of the Institute.

e. Whenever I have used materials (data, theoretical analysis, figures, and text) from other sources, I have given due credit to them in the text of the thesis and giving their details in the references.

f. Whenever I have quoted written materials from other sources, I have put them under quotation marks and given due credit to the sources by citing them and giving required details in the references.

ABHILASH PATEL

ACKNOWLEDGEMENTS

This thesis is one of my proud possession and it wont be in its final form without the help of others.

First, I express my sincere gratitude to my supervisor, Dr. Sandip Ghosh for his valuable guidance and suggestions throughout the work. I also thank him for his motivation, making himself available at the time of need, bearing me with my silly doubts without loosing patience .

I also express my earnest thanks to the Prof. Anup Kumar Panda, Head of the Department of Electrical Engineering, NIT Rourkela and Prof. Bidyadhar Subudhi, Coordinator, Control and Automation, for providing all the possible facilities towards this work. Also, thanks also to other faculty members in the department for the course work which established my foundation for research.

I thank Mr. Abhinav Kumar Singh, PhD, Imperial College London for his help in simulating new England system.

I want to thank friends from here, for bearing me two years and giving such love. Thanks friends for making my stay memorable.

My warmest thanks go to my family for their support, love, encouragement and patience. and at the last from Einstien's words:

Thanks to those who said NO !! because of them I did it myself.

Abhilash Patel

Rourkela

Abstract

One of the major issues in an interconnected power system is the damping of the inter-area oscillations which significantly reduces the power transfer capability. Though conventional controllers have been used such as power system stabilizer (PSS) to stabilize the local oscillations, these are not efficient to provide adequate damping to the inter-area modes. Advances in Wide-Area Measurement System (WAMS) makes it possible to use the information from geographical distant location to improve power system performances. A speed based Wide-area Damping Controller (WDC) provides supplementary control signal through the exciter of selected machine. The controller takes local and remote speed deviation signal as feedback. Here, geometrical measures for controllability and observability is performed to select the feedback signals and controller location. However, obtaining the remote signal may introduce a time-delay which may degrade the system performances or may even lead to instability. Here, depending upon feedback, two type of configurations are illustrated i.e. synchronous and non-synchronous. The effect of time-delay is studied for both the configurations. To consider the time-delay in the design stage, it is modeled with 2^{nd} order Pade approximation. The controllers are synthesized with an objective of H_∞ control with regional pole placement. Performances for both the type of feedback configurations are evaluated. To show the effectiveness of the designed controllers, two case studies have been taken up a 4 machine system and another 10 machine system. It has been found that with WDC the oscillations died out quickly. Also, study illustrated that a non-synchronous feedback performs better compare to synchronous feedback WDC.

Key words: Damping Controller, Wide-Area Control, Time-delay, Synchronization, Wide-Area Measurement System.

Contents

List of Symbols and Acronyms

List of Symbols

δ	:	Rotor angle of the machine
$\Delta\omega$	:	Speed deviation of the machine
H	:	Inertia constant
$\|\|X\|\|$	:	Euclidean norm of a vector or a matrix X
T'_{do}, T''_{do}	:	Open circuit transient and subtransient d-axis time constant
T'_{qo}, T''_{qo}	:	Open circuit transient and subtransient q-axis time constant
$< (\leq)$	:	Less than (Less than equal to)
$> (\geq)$	:	Greater than (Greater than equal to)
X^T	:	Transpose of matrix X
X^{-1}	:	Inverse of X
T_e	:	Electrical torque
T_m	:	Mechanical torque
E'_q	:	Transient emf due to field flux linkages
E'_d	:	transient emf due to flux linkage in q-axis damper coil
X_d,X'_d and X''_d	:	Synchronous, transient and sub-transient reactances along the d-axis
X_q,X'_q and X''_q	:	Synchronous, transient and sub-transient reactances along the q-axis
E_{fd}	:	Field excitation voltage
X_{ls}	:	Armature leakage reactance.
$\|X\|_\infty$	:	$\sup_w X(w)$
$X > 0$	:	Positive definite matrix X
$X \geq 0$	:	Positive semidefinite matrix X
$X < 0$	:	Negative definite matrix X
$X \leq 0$	:	Negative semidefinite matrix X

List of Acronyms

ARE	:	Algebraic Riccati Equation
ARI	:	Algebraic Riccati Inequality
LMI	:	Linear Matrix Inequality
LDC	:	Local Damping Controller
WDC	:	Wide-area Damping Controller
WAMS	:	Wide-Area Measurement System
PDC	:	Phasor Data Concentrator
PSS	:	Power System Stabilizer
AVR	:	Automatic Voltage Regulator
LSI	:	Loop Selection Index
MIMO	:	Multiple Input Multiple Output
SISO	:	Single Input Single Output
PMU	:	Phasor Measurement Unit

List of Figures

CHAPTER 1

Introduction

1.1 Overview and Motivation

With the growing need of power demand and geographical constraints on building new transmission lines, transfer of the huge amount of power over a long line without sacrificing stability is a key issue to study. Stability of power system has been considered as a critical problem for the operation since the beginning of last century. Lack of stability caused the blackouts in the past illustrated the value of the study. With power system deregulation, generation system now operates close to their limit. This makes the system be in stressed condition and inherent low damping of the system may not suffice to retain the system stability. Further, in the run of non-conventional energy resources, system damping is less than earlier due to the use of low inertia resources[32]. Also, unscheduled power generation by these resources introduces disturbance to the system. Following a disturbance, oscillation always occurs in power system due to the presence of the various dynamical components. With the absence of proper control, these oscillations may grow in nature and may lead to loss of synchronism. The near-to-failure event in ERCOT on February 26, 2008, is an example of such a situation.

As power system has evolved considerably, different forms of power system instability have emerged owing to the continuing expansion in interconnections, the application of new sophisticated technologies and controls in the power system. Depending upon the

physical parameters under study, stability issue is divided into three categories – i) Rotor Angle Stability ii) Frequency Stability and iii) Voltage Stability. As power system is highly nonlinear in nature, stability study also depends upon the magnitude of disturbances. So as per disturbance scale stability is two types – i) Small Signal Stability ii) Transient Stability. The former considers the effect of a small change in the system such as a change in load demand, change in mechanical input whereas later deals with disturbance such as a fault in lines, loss of the generator[38]. Here, small signal stability issue is the point of interest. Lack of small signal stability leads to growing nature of low frequency oscillations. Power system oscillation occurs with different modes like swing modes, exciter modes, torsional modes etc. Swing modes can be categories into two types – 1)Local Mode 2) Inter-area Mode. Intra-plant oscillations or when a generator oscillates against the generators tightly coupled with it from the same area, it is consider as local mode. Frequency of such modes are generally from 1 Hz to 3 Hz. When a group of generators from an area oscillates against another group of generators from another area connected over long transmission lines called as inter-area mode. It has a frequency from 0.1 Hz to 0.9 Hz generally. Inter-area modes may be caused by either high-gain exciters or heavy power transfers across weak tie-lines. A fast acting voltage regulator enhances the synchronizing torque component and also improve the transient stability, but sacrifices damping torque component[38], which results in sustained oscillations in the power system. The occurrence of such low frequency modes have been observed in , as 0.2 Hz in the western North-American power system[43], 0.6 Hz in the Hydro-Quebec system[22], in Brazil of 0.15-0.25 Hz [30] and 0.19-0.36 Hz in Europe [44]. In Indian grid low frequency oscillation with mode frequency of 0.5 Hz (0.45 Hz-0.55 Hz) was observed during the disturbance at Buddhipadar, Sterlite and IBTPS, oscillations of 0.49 Hz (0.45-0.55 Hz) was observed in the NEW grid during the forced outage of DSTPS Unit 2, as 0.2 Hz is also observed in the SR grid while taking Simhadri Unit-2 (500 MW) in service. This case presents a situation when LFO appeared while synchronizing a generating unit in the grid[39]. The recent 2003 blackout in eastern Canada and US was equally accompanied by severe 0.4 Hz oscillations in several post-contingency stages [3]. The 1996 and 2000 WECC blackout were also due to poor damped inter-area modes[35]. Similarly, India's 2012 blackout caused by oscillation from the heavy transfer of power through weak tie-line between Northern grid and Western grid[1]. Where inter-area modes of 0.35 Hz, 0.68 Hz, 0.53 Hz, 0.71 Hz have been observed which have near to zero damping.

Conventionally a damping controller is used (also called as Power System Stabilizer (PSS)) to damp out these oscillations by providing damping torque component through exciter. PSSs are used over the decades to control these oscillations. Usually, PSS is tuned as decentralized controller considering only local dynamics. A speed deviation based PSS takes feedback of speed deviation from local generator only. As PSSs use the local signal as input, which have low observability of inter-area oscillations so it performs poorly with inter-area oscillations. It has been illustrated that sometimes an inter-area mode may be well-observable from one area and be effectively controllable from another remote area[14]. Lack of global observability in Local Damping Controller (LDC) limit the performance over inter-area modes in the system. Hence power transfer capability in the system can't be improved significantly and recently, the power systems are pushed to operate near to design limits and with more uncertainty in the system, which makes the control of power systems more challenging than ever.

A more flexible and suitable environment has been developed with the recent progress in time synchronizing techniques, along with the computer-based technique, to estimate phasors in real time. With the worldwide deployment of phasor measurement unit (PMU), better dynamic data are available for monitoring and control[37]. Signals from a remote location are also available for designing a controller with better performance. The availability of remote signals can overcome the aforementioned shortcoming of lacking observability and provide flexibility to damp a special critical inter-area oscillation mode of power systems. To achieve the same performance, a local controller requires much more gain compared to the wide-area controller. This large control action can push the system to its limit and finally loss of feedback action. It is reported that a wide-area controller 4 to 20 times more efficient technically than the local controller[24].

Use of WAMS provides better dynamic data of the power system, but the involvement of remote signal arises some new challenges such as time-delay or latency. In wide-area control system transmitting signals from PMUs to PDC, and than back to generators involve some time-delays. The transmission delays depend upon various factors such as communical link, protocol, and traffic. Also, computational delays such as processing of signals and synchronization added an extra delay in the signals. In the Western Electricity Coordinating Council(WECC) for fibre optic cable delays reported as 25 ms to where as for satellite communication link delays ranges up to 250 ms. In [11] reported a time delay

of 150 ms in Nordic power system and [47] reported a delay of 100 ms for the Chinese power system. Indian WAMS reported a time delay of 250 ms in the report [39]. Different amount of delays is reported in the literature for WAMS system. The time delay in a system introduces infinite number of poles in the system with the right-hand zeros. So, a time delay in the system may reduce the damping of the system or even may also lead to instability [46]. It has also been reported that delay in obtaining signals may lose the synchronism in power system[45].Both communication delay and operational delay plays a vital role on system performances. Delays due to communications network range from few millisecond to orders of hundred millisecond depending upon bandwidth and protocol of communications[34]. A major part of the operational delay is due to synchronization of signals which involves receiving and resolving PMU data packets and synchronization of the data with respect to the GPS time-stamp[52].

A speed based Wide-area Damping Controller (WDC) takes the speed deviation signal as feedback from the power system. The measurements from the PMUs are sent to PDC and then to the controller. Depending upon feedback signal coming to the controller, the configuration can be said as *Synchronous* or *Non-Synchronous*. It is well known that inter-area mode is well observable in speed difference signal from two areas, so it is suitable to be feedback for the controller. When synchronized signal is fed to the controller, local and remote signals are matched with respect to time-stamp. An equal amount of time delays will be induced to both the signals. However, instead of fetching both the signal, one can opt for non-synchronised feedback. In this case, the only remote signal is to be obtained from PDC, so no time synchronization is needed. In this case delay in the local signal will be negligible, also delay in the remote signal will be less as no synchronization is being processed.

1.2 Literature Review

The field of WAMS is extended from only monitoring to be used in control application recently. Several design methods have been illustrated in the past to address the problem of power system oscillation control using WAMS technology. Fouad a pioneer in Power System Control in 1996 published a paper [2] establishes ground for wide area control work. Where a two level controller is designed based upon phase compensation method

from mode residue. Also, It has been reported in [23, 54, 55] of a lead-lag compensator. In reference [23], a decentralized/hierarchical structure with two loop PSSs is proposed. A wide-area damping controller is used to provide additional damping to local ones. To tune the loops a sequential optimization procedure is adopted. Design of lead-lag compensator is simple as it is designed in the similar manner of conventional PSS i.e. linear model of fixed operating conditions. Though it is easy to design and implementation but it lacks the important issue of robustness. It performs non-uniformly with varying operating conditions.

To cope with varying operating conditions adaptive control methods play good role for wide-area controller design as in [7, 53, 10, 5, 4, 15, 26]. . In [4, 5] a feedback linearization controller is developed which have the ability to self-tuning of its parameter based upon neural networks. In [15] a pole shifting controller is proposed where the system is identified using a recursive least square algorithm. In [7] multiple model base adaptive controller is proposed where as [6] illustrated model reference approach for adaptive control. Also, rule base control to suited with the adaptability are proposed in [19] based on fuzzy logic. The model self-tuning adaptive controls require consistent excitation for system dynamic model to identify the model which causes undesired disturbances in the system. The data-driven adaptive controls, despite being model free, depend on large disturbances to train parameters of a controller and the training procedure may encounter convergence problems.

Moving towards robustness LQG controllers are illustrated in [57] as a wide-area damping controller. It based on minimization of a cost function that penalizes states deviation and minimize control effort. An LTR scheme is used to achieve guarantee robustness in [57]. Also LQR scheme is applied in [41]. With the development of H_∞ control method in control theory has shown superiority to achieve robustness compared to any methods coexisted. H_∞ loop shaping approach along with regional pole placement is illustrated in [28]. In [28], loop shaping method is used as normalized LMI framework to achieve multiple objectives. In [56, 9] the design of H_2/H_∞ mixed sensitivity with regional pole placement controller is proposed. The controller is synthesized to minimized weighted sensitivity where the system critical mode needs with the wide area controller needed to be places a pre-specified region in left half plane ensuring the dynamic performance. But the developed controller is MIMO in nature, which gives threat to coupling of modes and complex synthesis problem.

All the above-mentioned methods ignore the effect of delays and have not considered during the design stage. However, fetching information through shared networks introduces

time-delay. The effect of delay has been studied in [16, 31]. Several works address the time delays in wide area control loop explicitly[48, 49, 50, 51, 33, 18, 8, 29].A model-free fuzzy controller, based upon operator experience rule base, has been designed in [33]. In this, the output membership functions are shifted in a manner to compensate the effect of the delay. A lead-lag compensator to compensate the phase is proposed in [49, 50] where the gain of the compensator is calculated from a tradeoff between delay margin and damping. To handle the uncertainty in delay [18] proposed a linear fractional transform model to be used in H_∞ control framework. Also, predictor based approach also have been used in [48, 51, 8, 29],where[8, 29] uses unified smith predictor to overcome minimum damping issue with classical smith predictor. In [48, 51] uses generalized predictive control along with RLS base model identification to make system adaptive in nature.

1.3 Objectives

Here, primary goal is to improve the dynamics of power system and towards it, a controller is to be synthesized. To achieve the goal following objectives need to satisfied:

- A model should be developed to capture required dynamics only rather than accurate complex model but no practical use. An analysis is to be performed for characterization of the system.

- As the obtained model can be of large order, which gives complexity in the design. So the model of the system is to be reduced such as it retain the input-output behavior at desired frequency range.

- Implementation of PMUs is costly due to its hardware and network requirement. One needs to minimize the number of signals needed for the operation.

- Suitable controller is to be synthesized to improve the damping of inter-area modes of the system. As power system is varying in nature so the controller should be able to handle such uncertainty in operating conditions.

- Obtaining wide-area signals involve time-delay which may deteriorate the system performance. So appropriate approach has to be taken to handle such delays.

1.4 Organization of the Thesis

The thesis is organized as follows:

Chapter–1) It gives a introduction to the problem and also discusses the earlier works that have been done on same line of objectives.

Chapter–2) The system modeling is illustrated in this chapter. A composite model is developed from the model of subsystem. Also, offline modal analysis is presented. How one can minimize the signals requirement is also answered in between. At last, it talks about model order reduction as the power system obtained model is too large order in nature.

Chapter–3) It gives the essential control theory needed to design the controller. The chapter begins with the formalization of synchronous and non-synchronous configuration. Then it discusses H_∞ control and regional pole placement objectives in LMI framework.

Chapter–4) Here, two case studies are taken to illustrate the objectives, one a 4 machine system and another 10 machine system. Results have been shown in step wise manner and appropiate discussions have been made. How a non-synchronous feedback works better than a conventional synchronous feedback is illustrated.

Chapter–5) This chapter gives conclusion to the work. Also provide a guideline for future work.

CHAPTER 2

Power System Modeling for Stability Studies

2.1 Small Signal Model of Power System

Non-linearity and large scale complexity these are two things which makes power system modelling a difficult task. The theory of nonlinear system can be used for stability analysis but with the such large order it is a cumbersome process. As power system is a largest complex plant possible, different dynamical phenomena with different characteristics occurred in power system. Its almost impossible to develop a model that can capture or describe all dynamics and still being of practical use. Depending upon interested particular investigation one has to develop a mathematical model that captures correctly particular dynamic phenomena. As power system is large scale, developing a composite model is suitable, where system is divided into different subsystem and relation between them is expressed linearly as algebraic equations[42]. As interested phenomena here being small signal stability with use of singular perturbation theory we can obtain differential algebraic equations (DAE) of the subsystem. By modeling the network as algebraic equation, a complete model can be developed. There are various components used in power system but some are important for stability studies.

2.1.1 Synchronous Machine

All the generators of the power system are represented using the sub-transient models with four equivalent rotor coils as per the IEEE convention. The slow-dynamics of the governors are ignored, and the mechanical torques to the generators are taken as constant inputs. Standard notations are followed in the following differential equations which represent the dynamic behavior of the generator [38]

$$
\begin{aligned}
\frac{d\delta_i}{dt} =& \omega_B\left(\omega_i-\omega_s\right)=\omega_B S_{mi}\\
2H_i\frac{dS_{mi}}{dt} =& \left(T_{mi}-T_{ei}\right)-D_iS_{mi}\\
T_{ei} =& {E_{di}}'I_{di}\frac{X''_{qi}-X_{lsi}}{X'_{qi}-X_{lsi}}+{E_{qi}}'I_{qi}\frac{X''_{di}-X_{lsi}}{X'_{di}-X_{lsi}}\\
&+I_{di}I_{qi}\left(X''_{di}-X''_{qi}\right))+\psi_{1di}I_{qi}\frac{X'_{di}-X''_{di}}{X'_{di}-X_{lsi}}+\psi_{2qi}I_{di}\frac{X'_{qi}-X''_{qi}}{X'_{qi}-X_{lsi}}\\
I_{qi}+jI_{di} =& \frac{1}{R_{ai}+jX''_{di}}\\
&E'_{qi}\frac{X''_{di}-X_{lsi}}{X'_{di}-X_{lsi}}+\psi_{1di}\frac{X'_{di}-X''_{di}}{X'_{di}-X_{lsi}}-V_{qi}+\\
&j\left({E_{di}}'\frac{X''_{qi}-X_{lsi}}{X'_{qi}-X_{lsi}}-\psi_{2qi}\frac{X'_{qi}-X''_{qi}}{X'_{qi}-X_{lsi}}-V_{di}+E'_{dci}\right)\\
T'_{ci}\frac{dE'_{dci}}{dt} =& I_{qi}\left(X''_{di}\right)-E'_{dc}\\
T'_{qoi}\frac{dE'_{di}}{dt} =& -E_{di}\left(X'_{qi}-X'_{qi}\right)\\
&\left\{-I_{qi}+\frac{X'_{qi}-X''_{qi}}{\left(X'_{qi}-X_{lsi}\right)^2}\left(\left(X'_{qi}-X_{lsi}\right)I_{qi}-E'_{di}-\psi_{2qi}\right)\right\}
\end{aligned}
\tag{2.1}
$$

Here, the subscript i refers to the i^{th} generator; δ is the rotor angle in radians; $\omega_B$is the rotor base angular speed in radians per second; H is the inertia constant in seconds; T'_{do} and T''_{do} are the d-axis open circuit transient and sub-transient time constants, respectively; T'_{qo} and T''_{qo} are the q-axis open circuit transient and sub-transient time constants, respectively; and T_c is the time constant for the dummy rotor coil (which is usually taken as 0.01 seconds). Rest of the variables are in per unit (p.u.): ω is rotor angular velocity; ω_S is the synchronous angular velocity; S_{mi} is the slip; T_m is the mechanical torque; T_e is the electrical torque; D is the machine rotor damping; E'_q is the transient emf due to field flux

linkages; E'_d is the transient emf due to flux linkage in q-axis damper coil; ψ_{1d} and ψ_{2d} are the sub-transient emfs due to d-axis and q-axis damper coils, respectively; E_{fd} is the field excitation voltage; E'_{dc} is the transient emf across the dummy rotor coil; I_d and I_q are the d-axis and q-axis components of the stator current, respectively; V_d and V_q are the d-axis and q-axis components of the stator terminal voltage, respectively; X_d,X'_d and X''_d are the synchronous, transient and sub-transient reactances, respectively, along the d-axis;X_q,X'_q and X''_q are the synchronous, transient and sub-transient reactances, respectively, along the q-axis; R_a is the armature resistance and X_{ls} is the armature leakage reactance.

2.1.2 Excitation System

Usually generators are equipped with a excitation system to provide dc field current to set up essential flux. The functional block diagram for excitation system is given in Fig.(2.1.2). The automatic voltage regulator (AVR) in the exciation system control the voltage profile. The voltage transducer acts as filter to feedback the terminal voltage. Transient gain reduction block is used reduce the gain at high frequency to retain stability, However, when PSS is used, its not necessary to use. Excitation system can be DC, AC and static. IEEE provides a standard to model the excitation system for stability studies citekundur03. The model for static excitation sytem can be given as:

$$\begin{aligned} T_A\frac{dE_{fd}}{dt} &= K_A\left(V_{ref}+V_s-V_r\right)-E_{fd}, \\ T_r\frac{dV_r}{dt} &= V_t-V_r, \end{aligned} \tag{2.2}$$

where E_{fd} is the field excitation voltage, T_r is the voltage transducer time constant, V_t is the terminal voltage i.e. output of the generator, V_r is the filtered voltage,K_A is the regulator gain, T_A is the regulator time constant, V_{ref} is the voltage reference.

2.1.3 Power System Stabilizer

Power System Stabilizer (PSS) is embedded in the excitation system to stabilize the power system from oscillation. They are tuned as decentralized manner and takes feedback of local signal only. Basic function of PSS is to provide supplementary signal through exciter to act as damping torque component by providing proper phase compensation as shown in Fig. 2.1.3. It can take speed, frequency or power as feedback. K_{pss} is the gain provided

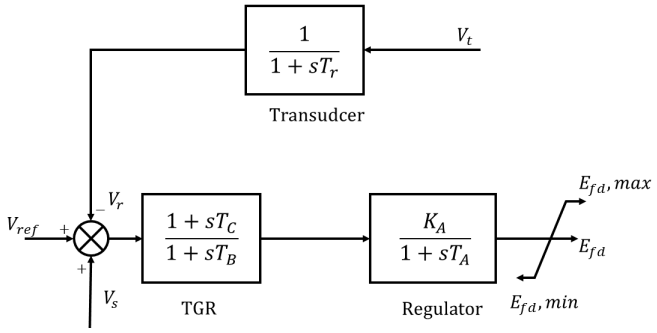

Figure 2.1: Functional block diagram of excitation system

for amplifying damping signal. Usually, high pass washout filter is used to avoid effect of other modes to action of PSS. The model of PSS can be written as:

$$G(s) = K_{pss} \frac{sT_w}{1 + sT_w} \frac{1 + sT_1}{1 + sT_2} \tag{2.3}$$

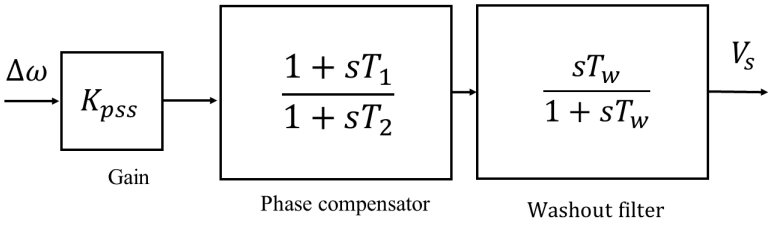

Figure 2.2: Functional block diagram of power system stabilizer

2.1.4 Load and Network Interface

The modeling of loads in stability studies is a complex problem due to the unclear nature of aggregated loads. Load models are typically classified into two broad categories: static and dynamic. The loads can be modeled using constant impedance, constant current and constant power static load models. Constant impedance load model is a static load model where the real and reactive power is proportional to the square of the voltage magnitude. It is also referred to as constant admittance load model. Here, such model is considered for stability studies.

Network balance equations is written as algebraic equations and it is needed to trans-

form all system dynamics into common reference frame. To do so, currents and voltages of the generators are needed to rotate δ.

$$\begin{aligned} I_{Qi} + jI_{Di} &= (I_{Qi} + jI_{Di})\, e^{j\delta i}, \\ V_{Qi} + jV_{Di} &= (V_{Qi} + jV_{Di})\, e^{j\delta i}. \end{aligned} \tag{2.4}$$

In order to incorporate generator admittance, it is represented as current injecting source in network, given by

$$I_{gi} = (I_{Qi} + jI_{Di}) + Y_{gi}V_{gi},$$

where $Y_{gi} = \frac{1}{R_{ai}+jX''_{di}}$. Admittance matrix is given by $diag\,[Y_{G1}, Y_{G1}, ...Y_{GN}]$ where N is the total bus nodes, where $Y_{Gij} = 0$ if j^{th} node is not connected to i^{th} generator and $Y_{Gij} = y_{gi}$ if j^{th} node is connected to i^{th} generator.

Similary one can define load admittance matrix Y_L where loads are considered as constant impedances. The network shunt admittance matrix Y_N is build using line impedance and augmented with Y_G and Y_L to give $Y_{aug} = Y_N + Y_G + Y_L$. So, Z_{aug} can be found out by inversing Y_{aug}

2.2 Modal Analysis

Once the system dynamics has obtained, a linear model is to be obtain for analysis and controller synthesis process. The dynamics have to be linearized around an equilibrium point by singular perturbation theory [38]. Consider the system dynamics as:

$$\begin{aligned} \dot{x} &= f\,(x, z, u)\,, \\ 0 &= g\,(x, z, u)\,, \\ y &= h\,(z, z, u)\,, \end{aligned} \tag{2.5}$$

where f,g,h are function vectors of differential, algebraic and output equations. A equllibrium pint can be obtained by solving the load flow and linearizing around the equllibrium

point (x_0, z_0, u_0),

$$\begin{aligned} \Delta\dot{x} =& \frac{df}{dx}\Delta x + \frac{df}{dz}\Delta z + \frac{df}{du}\Delta u, \\ 0 =& \frac{dg}{dx}\Delta x + \frac{dg}{dz}\Delta z + \frac{dg}{du}\Delta u, \\ \Delta y =& \frac{dh}{dx}\Delta x + \frac{dh}{dz}\Delta z + \frac{dh}{du}\Delta u. \end{aligned} \tag{2.6}$$

Eliminating algebraic Δz from (2.6),

$$\begin{aligned} \Delta\dot{x} &= A\Delta x + B\Delta u, \\ \Delta y &= C\Delta x + D\Delta u, \end{aligned} \tag{2.7}$$

where $A = \left[\frac{df}{dx} - \frac{df}{dz}\left(\frac{dg}{dz}\right)^{-1}\frac{dg}{dx}\right]$, $B = \left[\frac{df}{du} - \frac{df}{dz}\left(\frac{dg}{dz}\right)^{-1}\frac{dg}{du}\right]$, $C = \left[\frac{dh}{dx} - \frac{dh}{dz}\left(\frac{dg}{dz}\right)^{-1}\frac{dg}{dx}\right]$ and $D = \left[\frac{dh}{du} - \frac{dh}{dz}\left(\frac{dg}{dz}\right)^{-1}\frac{dg}{du}\right]$.

The eigenvalues of a matrix are the values obtained from nontrivial solution to the $A\phi = \lambda\phi$. For non-trivial solution

$$det\,(A - \lambda I) = 0$$

must satisfied. In a system free response is govern by linear combination of the eigenvalues of the state matrix. One can study the behaviour of the states by studying the eigen values. The eigen value with a finite frequency is called as Mode such as $\sigma \pm j\omega$. The stablity of the system depends upon σ, if it is in left half plane, mode is stable and for right hand side, mode is unstable, so as the system. For such mode frequency is given by $f = \frac{\omega}{2\pi}$ and damping is $\zeta = \frac{-\sigma}{\sqrt[root]{\sigma^2+\omega^2}}$. For any eigen value δ_i, there exist a coulmn vector ϕ_i which satisfies $A\phi_i = \delta_i\phi_i$ is called as right eigen vector. The right eigen vector of a mode is called as Mode Shape. Mode shapes give pictures of activities of states when the modes are excited and the scale of activity of a state x_k in the i^{th} mode is given by the elemnet ϕ_{ki} of right eigen vector ϕ_i. Participation factor is measure which provides relative participation of a state in a mode. Suppose P is matrix where P_i represents its i^{th} column. One can

obtain

$$P_i = \begin{pmatrix} P_{1i} \\ P_{2i} \\ \vdots \\ P_{ni} \end{pmatrix} = \begin{pmatrix} \Phi_{1i}\Psi_{i1} \\ \Phi_{2i}\Psi_{i2} \\ \vdots \\ \Phi_{ni}\Psi_{in} \end{pmatrix} \tag{2.8}$$

where $\Psi = \Phi^{-1}$ also called as left eigen vector. The element p_{ki} is a measure of the relative participation of k^{th} state variable in i^{th} mode. With the participation factor analysis, swing modes can be identified. If the sum of participation factor related $\delta_i, \Delta\omega$ to a mode is greater than participation from remain states than its called as swing mode. One can identify whether a mode is local or inter-area from its mode shape. Suppose mode shape of $\Delta\omega_i$ state is having phase difference nearly 180 to $\Delta\omega_j$ state associated with a mode, it means i^{th} machine is oscillating against j^{th} machine. So, if i^{th}, j^{th} machine belongs to same area, the mode associated with is called as Local Mode or if they belongs to different area the mode is called as inter-area mode.

2.3 Wide-Area Loop Selection

A model of the power system exhibit multiple inputs and multiple outputs. So, consideration of all of its makes the design procedure complex. Also, Due to the costs associated with the installations of PMUs, e.g. communication infrastructure costs, number of installed measurement devices should be minimised. For wide-area control a input-output pair can be selected such that it is more effective to inter-area mode. There have been different approaches mentioned in literature, but it appears that the approach for computing loop selection index based on geometrical approach is effective since it is not affected by scaling of the eigenvector, rather it is based on how input channel or output channel aligned to corresponding mode or eigen vector[17].

$$LSI_{mn} = \frac{|{b_m}^T v_l||c_n v_r|}{\|b_m\|\|v_l\|\|c_n\|\|v_r\|}$$

LSI_{mn} is the loop selection index corresponding to m^{th} input and n^{th} output combination, b_m is the input vector and c_n is the output vector corresponding to m^{th} input and n^{th} output respectively; v_l is the left eigen vector and v_r is right eigenvector of inter-area mode.

When there exist multiple modes, there may possiblity of trade off between LSI and interaction. One can opt for set of signals that have comparatively less effect to other modes

2.4 Model Order Reduction

A system such as power system have larger order due to large scale in nature. Modern controller methods such as H_∞ or LQG synthesize controllers at least order as same as the system or sometimes more than that due to the incursion of the weights. A Large order model gives rise to (i) large order of controller (ii) large computation time while synthesis of controller. One can opt for a lower order model which retains the input-output behaviour over the desired frequency range as the original model. There are large number of techniques available to reduce the order of the model [25]. One the simplest methods widely used is balanced truncation as discussed in [25]. It requires a state truncation of a system which is represented in balanced state space form, where controllability and observability grammians are equal and diagonal. Another method which is gaining importance is hankel norm methods. The Hankel norm is a induced norm from past input to future outputs. Keeping larger energy states of a system preserves most of its characteristics in terms of stability, frequency, and time responses [20]. Given a high order linear time-invariant model $G(s)$, we need to find out a low order approximation $G_r(s)$ such that the infinity norm of the difference i.e.$\|G - G_r\|_\infty$ is small. Depending upon the error bound it can be additive or multiplicative. If

$$\left\|G^{-1}(G - G_r)\right\|_\infty \leq \prod_{k+1}^{n} (1 + 2\,\sigma_i(\sqrt{1 + \sigma_i^2})) - 1$$

its called as multiplicative error bound whereas if

$$\|G - G_r\|_\infty \leq 2 \sum_{k+1}^{n} \sigma_i$$

it is called as additive error bound. For system with low damped modes, multiplicative error is more suitable.

2.5 Chapter Summary

This chapter briefly expressed the modeling and analysis of power system for small signal stability studies. Here, the system behavior is evaluated through modal analysis. To have a decentralized structure, wide-area loop selection is discussed. Finally, how to reduce the model order by using hankel norm for flexibility is illustrated.

CHAPTER 3

Wide-Area Controller Design

3.1 Introduction

Robustness is of crucial importance in control-system design because real engineering systems are vulnerable to external disturbance and measurement noise and there are always differences between mathematical models used for design and the actual system. Typically, a control engineer is required to design a controller that will stabilize a plant, if it is not stable originally, and satisfy certain performance levels in the presence of disturbance signals, noise interference, unmodeled plant dynamics and plant-parameter variations. A damping torque is generated by the controller by compensating the phase lag between AVR to machine, so the the torque should align in the direction of $\Delta\omega$. Suppose, a WDC is tune considering a weak line situation, may not work uniformly in other condition, cause as line reactance increases, the synchronizing torque also increases so as frequency of oscillation and thus phase lead requirement. Power System works in varying operating conditions making a complex dynamics to be presented as a mathematical model. So a robust control techniques comes handy in this situation. Oscillations in power systems are caused by variation of load, action of voltage regulator due to fault, etc. appear to damping controller these changes can be considered as disturbances on output y, the primary function of the controller is to minimize the impact of these disturbances on power system.

The objective behind the robust control is to provide control action that ensure the

stability and performance even with uncertainty in the system. Also, the modelling error must not effect the performance significantly with actual system. From all the availble methods existed for robust control H_∞ based technique is very popular and has been used very widely.

3.2 Consideration of Delays

System with wide-area control structure is shown in Fig.(**??**). Inter-area oscillations is well viewed as the difference of speed of the i^{th} and j^{th} generator from the two different areas(i.e. $\Delta\omega_{ij} = \Delta\omega_i - \Delta\omega_j$)[2]. Intuitively, this requires time-synchronization of the two signals and may easily be accomplished due to the deployment of PMUs for WAMS in modern power systems. This scheme is presented in Fig. **??** with the switch S positioned at 1. However, due to facilitating the synchronization, an equal amount of delays are introduced in the synchronized signal, whereas if the two signals are used without synchronization then the delay in the local signal is negligible. The case of using the non-synchronized signal, i.e. using the signals as and when available without the process of synchronization corresponds to the case when S is positioned at 2 in **??**. Analysis of system performance has been studied in[16] for both the configurations. Consider a linear system with state space representation

$$\begin{aligned} \dot{x}_p &= A_p x_p + B_p u_p, \\ y_p &= C_p x_p, \end{aligned} \tag{3.1}$$

is to be control with

$$\begin{aligned} \dot{x}_c &= A_c x_c + B_c u_c, \\ y_c &= C_c x_c, \end{aligned} \tag{3.2}$$

where $G_p(s) = C_p(s)(sI - A_p)^{-1}B_p$ represents the linearized power system model and the controller is $K(s) = C_c(s)(sI - A_c)^{-1}B_c$, u_p is the wide-area control signal fed to the exciter, y_p is the measured output considered here as speed deviation,x_p are the power system states,x_c is the vector of controller states.

Time-delay is modeled as 2^{nd} order Pade approximation in this work. From [16], it is illustrated a 2^{nd} order give the reasonably good handle of delay. State-space model of Pade

approximated delay term can be written as

$$\begin{aligned} \dot{x}_d &= A_d x_d + B_d u_d, \\ y_d &= C_d x_d + D_d y_d, \end{aligned} \tag{3.3}$$

where

$$A_d = \begin{bmatrix} 0 & 1 \\ \frac{-12}{{T_d}^2} & \frac{6}{T_d} \end{bmatrix} B_d = \begin{bmatrix} 0 \\ 1 \end{bmatrix} C_d = \begin{bmatrix} 0 & -T_d \end{bmatrix} D_d = \begin{bmatrix} 1 \end{bmatrix}.$$

Here, x_d represents the states of the Pade approximation, $u_d = y_p$ power system non-delayed output i.e. speed deviation signals, $y_p = u_c$ controller input or feedback i.e. delayed speed deviation signals.

Synchronous Feedback

When S is at 1, both local and remote signal are synchronized, so equal amount of time-delays are introduced in both the signals. A function block diagram is shown in Fig.4.1.8. State-space representation of closed-loop system can be written as:

$$\begin{aligned} \dot{x} &= A_1 x, \\ z &= C_p x_p, \end{aligned}$$

where $x = \begin{bmatrix} {x_p}^T & {x_d}^T & {x_c}^T \end{bmatrix}^T$ and

$$A_1 = \begin{bmatrix} A_p & 0 & B_p C_c \\ B_d C_p & A_d & 0 \\ B_c D_d C_p & B_c C_d & A_c \end{bmatrix}.$$

Non-Synchronous Feedback

When S is at 2, local signal is used as it is without waiting for synchronization so the delay is observed in remote signal only. A function block diagram is shown in Fig.4.1.8. From 3.1 where $C = \begin{bmatrix} {C_l}^T & {C_r}^T \end{bmatrix}^T$, C_l and C_r corresponds to local signal and remote signals

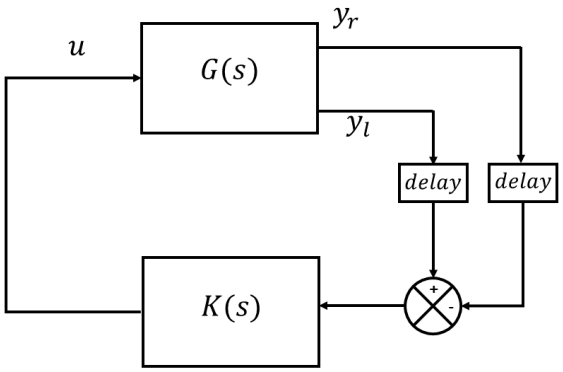

Figure 3.1: Control block diagram for synchronous feedback

respectively. Similarly state space representation of closed-loop system can be written as:

$$\dot{x} = A_2 x,$$
$$z = C_p x_p,$$

where $x = \begin{bmatrix} {x_p}^T & {x_d}^T & {x_c}^T \end{bmatrix}^T$ and

$$A_2 = \begin{bmatrix} A_p & 0 & B_p C_c \\ B_d C_r & A_d & 0 \\ B_c C_l + B_c D_d C_r & B_c C_d & A_c \end{bmatrix}.$$

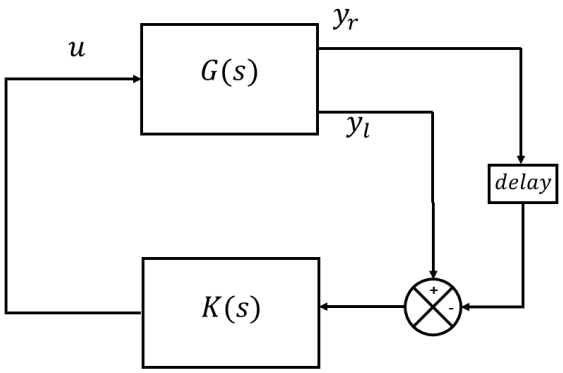

Figure 3.2: Control block diagram for non-synchronous feedback

3.3 H_∞ Control Synthesis

H_∞ is a functional family where functions are analytic and bounded in the right half plane. In other words, it can be said that H_∞ space consists of transfer function that has no pole in right half plane i.e. stable in nature.

In H_∞ control, objective is to minimize the H_∞ norm of certain closed-loop transfer function, that are related to stability and performance. A norm denotes size of signal or system and can be used a measure for the performance. From the block diagram **??**, the output can be written as $Y(s) = G(s)U(s)$. One can measure the performance in time domain with L_2 and L_∞ norm of $y(t),\ u(t)$. The L_2 norm of the signal $e(t)$ can be written as

$$\|e(t)\|_2 = \sqrt{\int_{-\infty}^{\infty} e(t)^T\, u(t) dt}.$$

Also called as Integral Square Error (ISE). Similarly L_∞ can be defined as

$$\|e(t)\|_\infty = \max_\tau(\max_i |e_i(t)|)$$

. The performance of SISO systems with feedback is influenced strongly by the variation of the open loop gain with frequency. The disturbance rejection and accuracy of tracking also depend on the open loop gain. In the multivariable case the concept of gain is replaced by the singular value of the transfer function matrix. They are also called principal gains. Similar to Bode plots of SISO systems, the singular values are plotted with frequency for a multivariable system.

Similarly to signal norm, performance can be measure with system norm of $G(s)$. H_∞ norm is one of such measureant. It provides gain of the system in worst case scenario. $\|G(s)\|_\infty = \sup_{u(t)\neq 0} \frac{\|y(t)\|_2}{\|u(t)\|_2}$ where $y(t)$ and $u(t)$ are the output and input. For stable system, $\|G(j\omega)\|_\infty = \sup_\omega |G(j\omega)|$ and for MIMO system $\|G(j\omega)\|_\infty = \sup_\omega \bar{\sigma}(G(j\omega))$. $G(j\omega)$ represents the gain from input to output of sinusoids of frequency ω and H_∞ is simply a measure of the largest factor by which any sinusoid is magnified by the system.

The control structure of a generalized plant is presented in 3.3. To achieve good performance, controller should reject disturbances and attenuate the effect of noise. From

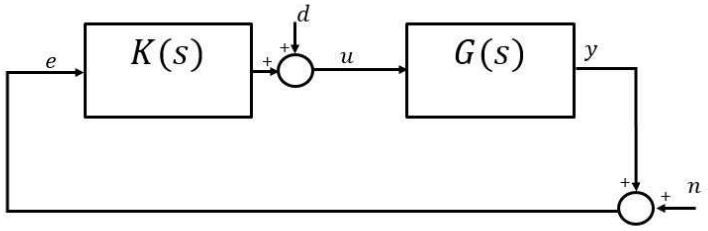

Figure 3.3: Generalized Control Plant

Fig.3.3, it can be written as in [20]

$$y = (1 + GK)^{-1}Gd + GK(1 + GK)^{-1}n, \tag{3.4}$$

where $(1 + GK)^{-1}$ is called as sensitivity function S and $GK(1 + GK)^{-1}$ is called as complementary sensitivity function T. To have a good disturbance rejection S should be minimum whereas to attenuate noise T should be minimum. For minimization index H_∞ index is chosen. There is certain limitation as T and S are complimentary to each other as $S + T = 1$. So, when we minimize S, T achieves the maximum value. One reformulate the objective with frequency dependent weight, which gives bound of S and T. It is well known that disturbances are of low frequency in nature whereas noises are of high frequency, so by using frequency-dependent weight one can set an objective without any trade-off. Considering H_∞ as performance measuring index ($\| \cdot \|_\infty$ is the H_∞ norm of the transfer function i.e. the supremum of its singular values over frequency, denoted as γ_∞), one can define the requirement as:

$$\left\| \begin{array}{c} W_1 S \\ W_2 SK \\ W_3 T \end{array} \right\|_\infty \leq \gamma, \tag{3.5}$$

where W_1 , W_2 and W_3 are suitable frequency dependent weight function and provides the flexibility of exploring the frequency based design trade-off between S and T. Usually W_1 is having transfer function of low pass filter and W_3 is of high pass filter. To avoid high control action, W_2 is used. W_2 is used to limit the control action at high frequency so as to avoid saturation and lose of stability, so a high pass filter is used or a constant is well

suited for the design. It is crucial for the designer to select appropriate weight function, but there is no systematic procedure available in the literature to achieve optimal weight functions. It is done based upon intuition and trial-error manner. One can put robust stability criteria for control synthesis from small gain theorem. Its a derived from Nyquist criterion. It states that the closed loop system will remain stable if a gain measure of the product of all transfer function matrices constituting the feedback path is less than unity.

A general block diagram showing objectives in the framework of H_∞ control is shown in Fig.3.4. The above objective can be written as generalized system [20]:

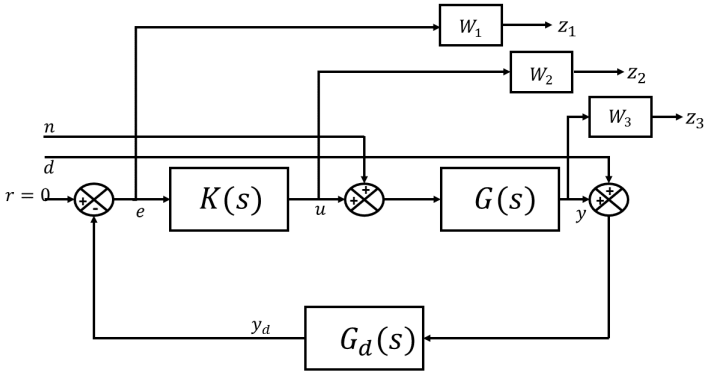

Figure 3.4: H_∞ control problem block diagram

$$\begin{bmatrix} z \\ y \end{bmatrix} = \begin{bmatrix} W_1 G_d G & W_1 G_d & W_1 G_d G \\ 0 & 0 & W_2 \\ G W_3 & 0 & G W_3 \\ G & 0 & G \end{bmatrix} \begin{bmatrix} d \\ n \\ u \end{bmatrix}, \tag{3.6}$$

where G is the system, G_d is the delay block, d is the disturbance, n is the noise in the signal, y is the ouput, y_d is the delayed output.

One can rewrite the above objective in Linear Matrix Inequalities (LMI) which is more computationally attractive and can be used in the framework as multi-objective control[12, 40]. Solving in LMI, avoids the pole-zero cancellation, also a low order controller can be synthesized. Considering the closed-loop system 3.2 now with exogenous signal w i.e.

disturbance d and noise n. it can be rewritten as

$$\begin{aligned} \dot{x} &= Ax + Bw \\ z &= Cx + Dw \end{aligned} \tag{3.7}$$

Now, A is stable and H_∞ norm of (3.7) is smaller than γ if and only if there exists a symmetric P satisfying

$$\begin{pmatrix} A^TP + PA & PB & C^T \\ B^TP & -\gamma I & D \\ C & D & -\gamma I \end{pmatrix} < 0 \tag{3.8}$$

However, involvement of controller parameter such as PA make the inequality 3.8 bi-linear one, using the variable transformation of [**?**] it can be expressed as LMI.

3.4 Regional Pole Placement

While H_∞ control addresses the frequency domain specification such as disturbance rejection and robustness effectively but it lacks the control over transient performance. Time domain performance requirement can easily be interpreted in terms of closed loop poles. Consider a closed-loop pole, $\sigma \pm j\omega$, where σ effects the damping and overshoot, where as ω represents speed of the response. Desired response can be achieved by forcing the closed loop poles of the system to be some particular values i.e. point-wise pole placement. Also, a region in left half plane can be specified for desired response, and control action can push the system poles to lie in the region.

An LMI region is any D region in the complex plane that can be defined as

$$D = \{z \in C : L + zM + \bar{z}M^T < 0\}$$

where $L = L^T$ and M are fixed real matrices. The matrix-valued function $f_D(z) = L + zM + \bar{z}M^T$ is called as characteristic function of D region .

Consider a system (3.1), if the poles or eigenvalues of A_p matrix lies in D region its called as D stable, and from lyapunov's extension[13], its possible if and only if a symmetric

postive definite matrix P exists such that

$$M_D(A, P) := L \otimes P + M \otimes (PA) + M^T \otimes (A^T P) < 0 \tag{3.9}$$

One can formulate different LMI regions, suitable to the need, Some are given below:

- α Region

  The α region is shown in Fig. 3.5, where all the poles lies left to a line at α parallel to $Y - axis$. Left half plane is a special case where $\alpha = 0$. The characteristic function for α stability region is:

  $$f_D(z) = 2\alpha + z + \bar{z}.$$

  One can opt for this region for ensuring stability and minimum settling time in terms of α.

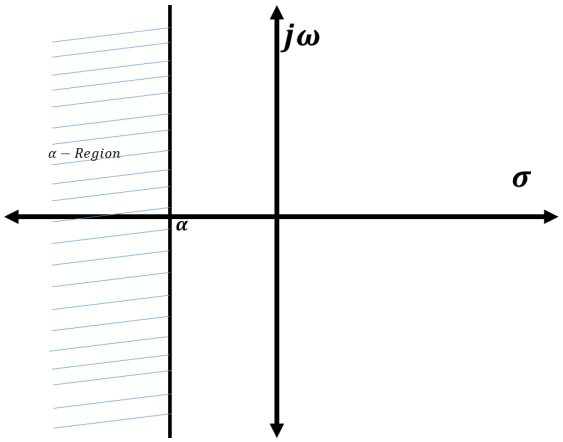

Figure 3.5: α LMI region

- Disk Centered Region

  For a disk region centred at (-q,0) with radius r, shown in Fig. 3.6, the characteristic equation is given by:

  $$f_D(z) = \begin{bmatrix} -r & q+z \\ q+\bar{z} & -r \end{bmatrix}$$

- Conical Sector Region To achieve minimum damping ratio, a conical sector is best suited, shown in Fig. 3.7. Characteristic function of conic sector with apex at origin

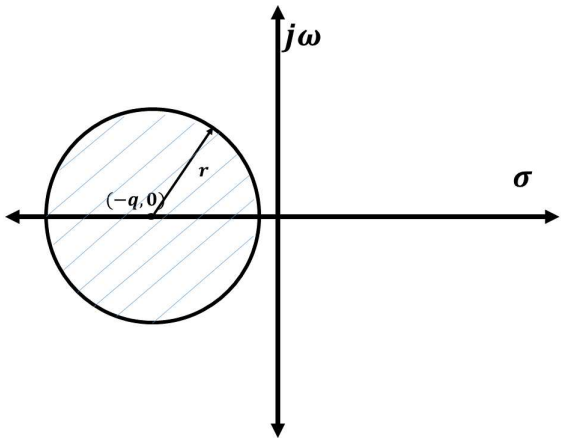

Figure 3.6: Disk centered LMI region

and inner angle of 2θ can be expressed as

$$f_D(z) = \begin{bmatrix} \sin\theta(z+\bar{z}) & \cos\theta(z-\bar{z}) \\ \cos\theta(\bar{z}-z) & \sin\theta(z+\bar{z}) \end{bmatrix}$$

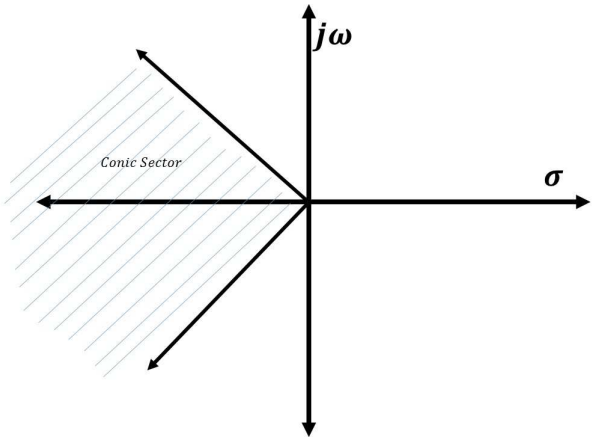

Figure 3.7: Conical sector LMI region

Pole clustering in LMI regions can be formulated as an optimization problem with robustness[13] or it can be fused with different performance constraints for multi-objective control[40, 12]. Different suitable LMI regions can be combined, forming a desired D region, which also be an LMI in nature.

3.5 Design Steps

The design procedure on this thesis can be summarized as below:

Step 1. Obtain a linearized model of the power system without wide-area loop.

Step 2. Once the linearized model is obtained, analyze the system modes with modal analysis and select suitable feedback loop for WDC. Reduce the model to suitable order for flexibility.

Step 3. Design a WDC with suitable design consideration. Here, H_∞ control with regional pole placement is considered.

Step 4. Estimate the delay for synchronous and non-synchronous feedback from time-stamped PMU signals. Approximate the delay with Pade 2^{nd} order.

Step 4. Design the WDCs for synchronous feedback and non-synchronous feedback. A comparison is done for performance evaluations.

3.6 Chapter Summary

This chapter presented the control theory for the synthesis procedure. After a brief introduction on the issue, system representation for synchronous and non-synchronous feedback are shown. Next, the H_∞ control objective is discussed and points were made why H_∞ control is suitable in power system design. Though it handle frequency domain specification very well, but it lacks control over transient performance. To overcome the issue, regional pole placement objective is embedded in the design. The synthesis procedure presented in LMI form. At last, over all design procedure is presented in step wise manner.

CHAPTER 4

Case Studies

4.1 Four Machine Eleven Bus System

4.1.1 System Description

The benchmark two-area system developed for study of inter-area oscillations [38] and used to demonstrate the effect of delay in the feedback loop. The system consisting of 11 buses

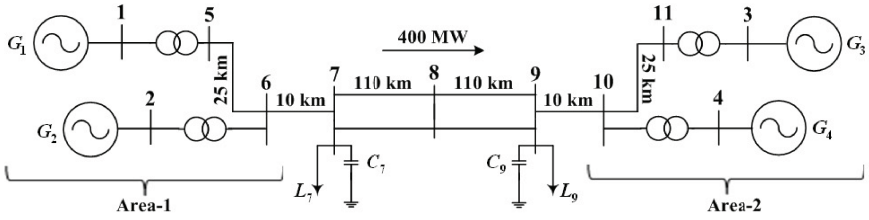

Figure 4.1: The 4 machines 11 buses study system[38]

and 4 generators is shown in Fig. 4.1. The two areas are connected by a weak tie-line. In present operating conditions a 400 MW power is getting transferred from area 1 to area 2. Each area of the system consists of two generators and each area equipped with a LPSS at G_1 and G_3 terminals to provide sufficient damping of local modes, however, as noted in [2], such local controllers are inefficient in improving inter-area damping. The nominal system parameters and operating point without any wide-area control are considered as it is given in [38].

4.1.2 Modal Analysis

The system is modeled in MATLAB-Simulink and linearized around operating point with the *linearize* command. The linearized model came as 58^{th} order. The modes of the system are then studied. To identify swing modes, participation factors of modes have been obtained as shown in Fig.4.2. In swing modes the states $\Delta\omega_i$ and $\Delta\delta_i$ of i^{th} generator should have higher participation compared to other states. In Fig.(4.2(a)), it is shown that $\Delta\omega_i$ and $\Delta\delta_i$ of all machines participating to M_1 mode whereas in Fig. 4.2(b), Fig. 4.2(c) only states from one area participating at a time. So here, modes M_1, M_2, M_3 are identified as swing modes.

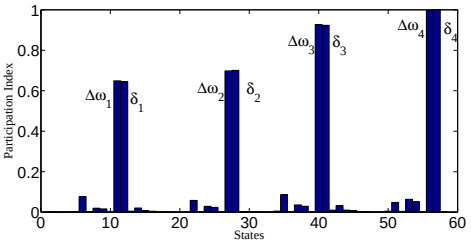

(a) M_1 mode

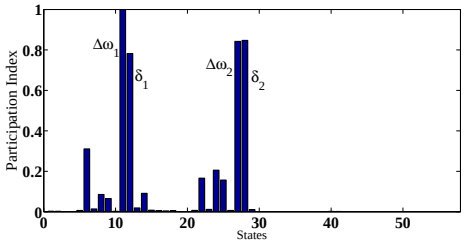

(b) M_2 mode

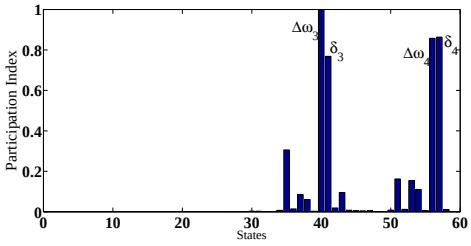

(c) M_3 mode

Figure 4.2: Participation factors of the three swing modes

Next, to identify local and inter-area in modes, mode shapes are plotted as shown in Fig.(4.3). From Fig.4.3(a), it is shown that G_1 and G_2 have mode shape opposite to G_3 and G_4, so M_1 is the inter-area mode. In $M1$, G_1 and G_2 will oscillate against G_3 and G_4. Also, it can observed that machine near to tie line have more activity compared to the distant machine in their area. From mode shape of M_2 as shown in Fig.4.3(b), it can be seen that G_1 oscillate against G_2. Though mode shape for G_3 and G_4 is presented in the Fig.4.3(b), it is not significanty visible as it is local mode of area 1. Similarly, from Fig.(

4.3(c)), one can observed G_3 is oscillating against G_4. Summary of analysis is presented in tabular manner in table 4.1.

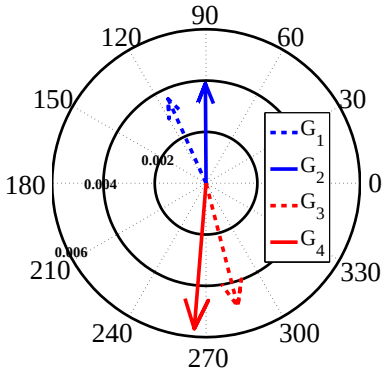

(a) M_1 Mode

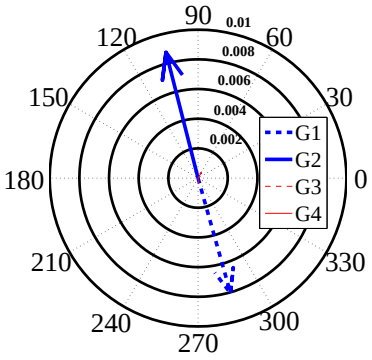

(b) M_2 Mode

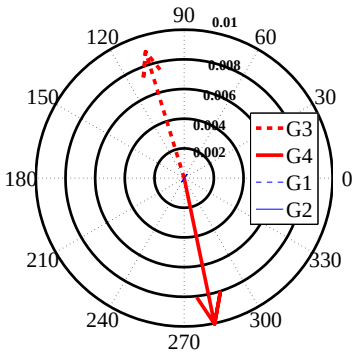

(c) M_3 Mode

Figure 4.3: Mode Shapes of the swing modes

Table 4.1: Swing modes of the system without WDC

Mode	Mode Shape	Frequency	Damping
M_1	Area-1 v/s Area-2	0.6223	0.08
M_2	G_1 v/s G_2	1.1395	0.24
M_3	G_3 v/s G_4	1.2112	0.20

4.1.3 Wide-Area Loop Selection

As mentioned earlier, inter-area mode are well observable in difference between the speed deviation of two machines located in the areas associated with inter-area mode. Also, one has to select location for the controller i.e. generator's excitation system, which is more effective to inter-area mode. Here a speed deviation based WDC is considered, so possible candidates for feedback signals are $\Delta\omega_{13}$, $\Delta\omega_{14}$, $\Delta\omega_{23}$, $\Delta\omega_{24}$. Loop selection index are calculated based on geometrical measures of controllability and observability as in [17]. The indexes are presented in tabular manner in 4.2. From 4.2, it can be concluded that $\Delta\omega_{24}$ and G_4 is suitable for input and output pair for the controller.

Table 4.2: LSI of the IO/OP signals

	$\Delta\omega_{13}$	$\Delta\omega_{14}$	$\Delta\omega_{23}$	$\Delta\omega_{24}$
G_1	1.2654	1.1813	X	X
G_2	X	X	1.3184	1.2182
G_3	1.33	X	1.2036	X
G_4	X	1.2990	X	**1.4502**

4.1.4 Model Order Reduction

The obtained system model is 58^{th} order which gives rise to (i) large order of controller (ii) large computation time while synthesis of controller. A H_∞ synthesis produces controller equal to plant's order plus order of weighting function, which is difficult to implement for large order. To address the problem, the model is reduced to lower order one i.e. 8^{th} order by *Hankel Model Reduction* method [20]. One can reduce the system order condition to reduced order and original order system frequency response matches in desired frequency range. Frequency response of original order and reduced order system is shown in Fig.4.4. Note that, reduced order system retain the inter-area mode M_1 and a local mode M_3 of the original system.

4.1.5 Controller Synthesis (Without Considering Delay)

With the reduced order model, the controller is designed. As a first case, no delay in the wide-area loop has been considered in the design. The controller is synthesized using H_∞ with regional pole placement. The weighting function for H_∞ design is considered as

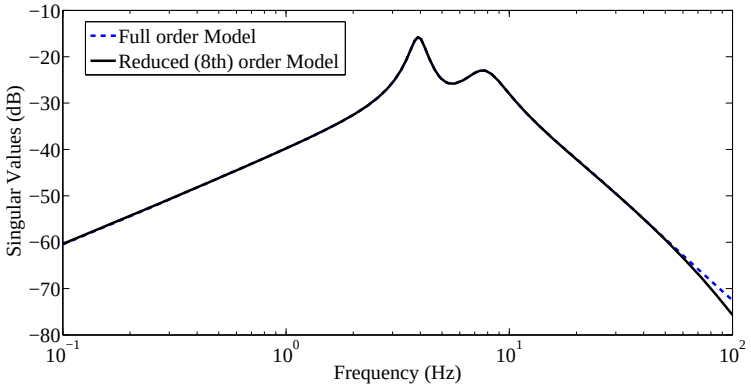

Figure 4.4: Singular value plot for full order and reduced order model

$W_1 = \frac{10}{s+10}$, $W_3 = \frac{10s}{s+10}$. So, S will be bounded by $\frac{1}{W_1}$ and T_3 will show integral action at high frequency due to W_3. To ensure minimum damping of 0.2, a conical region is selected as the desired LMI region. Here, to study the effect of local mode of an area, differences between the speed deviations of the machines from the area is considered i.e. $\Delta\omega_{12}$ to study oscillations in area-1. Similarly to study inter-area mode $\Delta\omega_{24}$ is considered.

The designed controller obtained as of 9^{th} order. The controller is further reduced to 5^{th} order by model reduction method. The frequency response of reduce order and full order controller is shown in Fig.4.5. Now, with the WDC damping of the inter-area mode

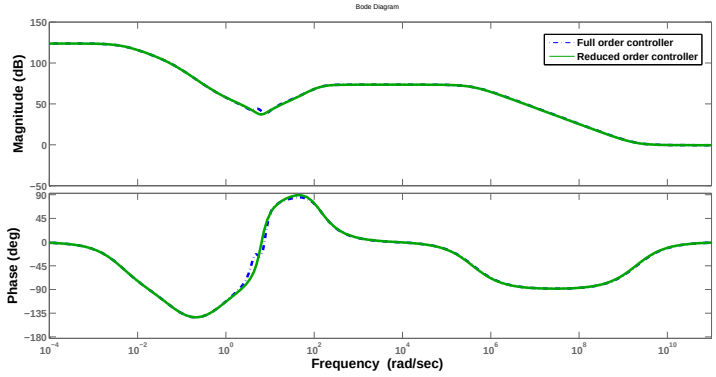

Figure 4.5: Bode plot of full order controller and reduced order controller

is improved from 0.08 to 0.253. The controller is validated through nonlinear simulation in Simulink. The effectiveness of both the both full-order controller and reduced-order controller are shown in Fig.4.6 in terms of inter-area oscillation. Without the wide-area loop, speed deviation is taking more than 10 *secs* to get settled, which is undesirable

following IEEE guidelines[27]. With the designed wide area controller, it can be seen that inter-area oscillations are died out quickly compared to not having the wide-area loop.

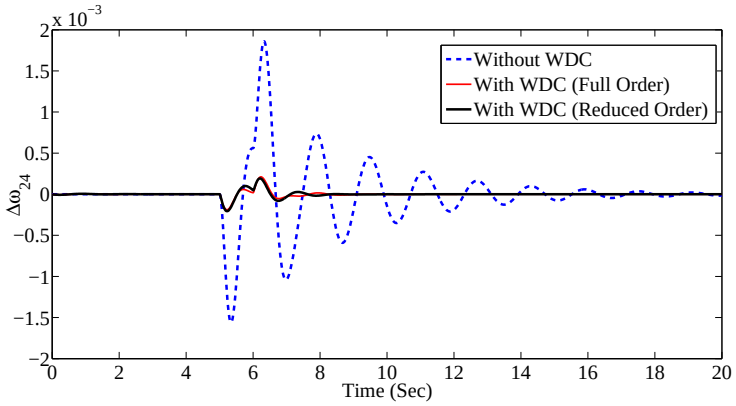

Figure 4.6: $\Delta\omega_{24}$ plot a) Without WDC b) With WDC (full and reduced order)

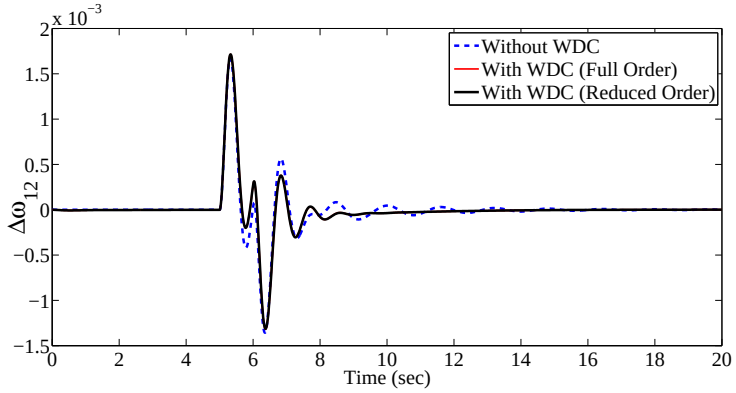

Figure 4.7: $\Delta\omega_{12}$ plot a) Without WDC b) With WDC (full and reduced order)

4.1.6 Robustness Analysis

To show the robustness, different operating conditions are considered as well as disturbance is considered in different path. Now, disturbance is added to the system from G_1 as pulse change in mechanical input for 0.2 *sec* of 0.05 magnitude. The speed deviations response corresponding to disturbance is shown in Fig. 4.8,4.9, where it can been seen that oscillations has been died out very soon with WDC compared to without WDC. The tie-line power is shown in Fig.(4.10). Also, varying operating conditions are considered where tie-line powers are 250 MW, 400 MW, 650 MW. The response to the disturbance is shown in Fig.4.12,4.11,4.13.

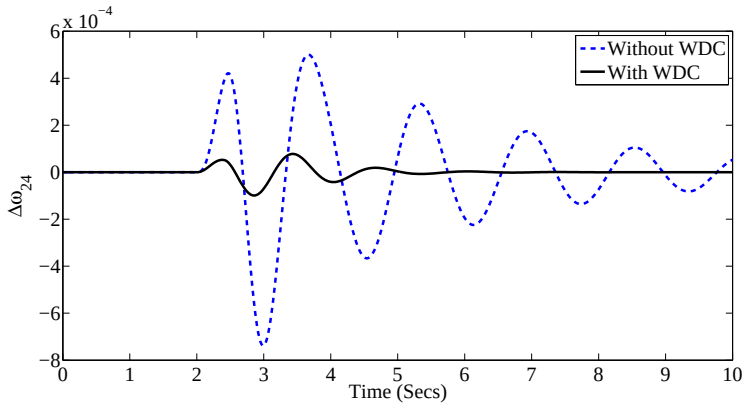

Figure 4.8: $\Delta\omega_{24}$ plot a) without WDC b) With WDC

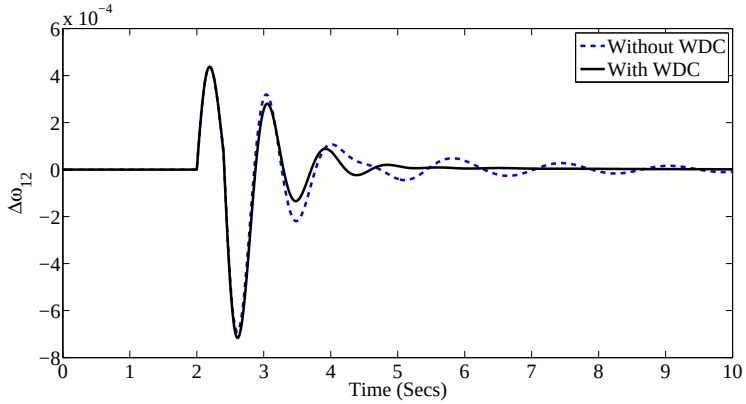

Figure 4.9: $\Delta\omega_{12}$ plot a) without WDC b) With WDC

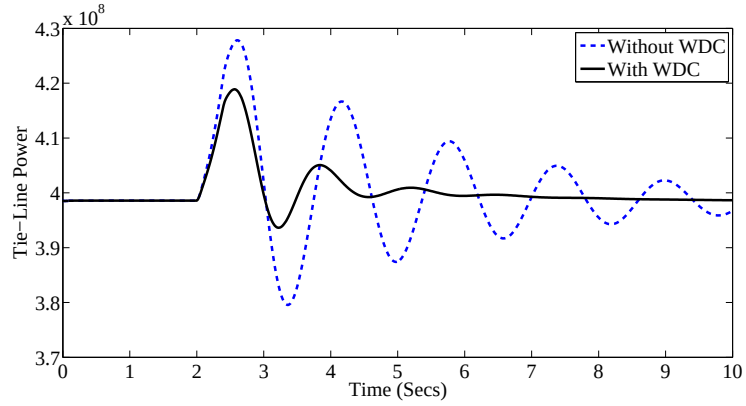

Figure 4.10: Tie-line Power plot a) without WDC b) With WDC

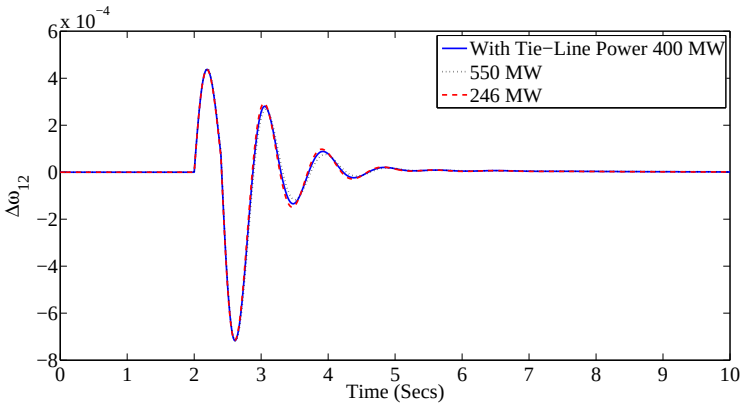

Figure 4.11: $\Delta\omega_{24}$ plot a) without WDC b) With WDC

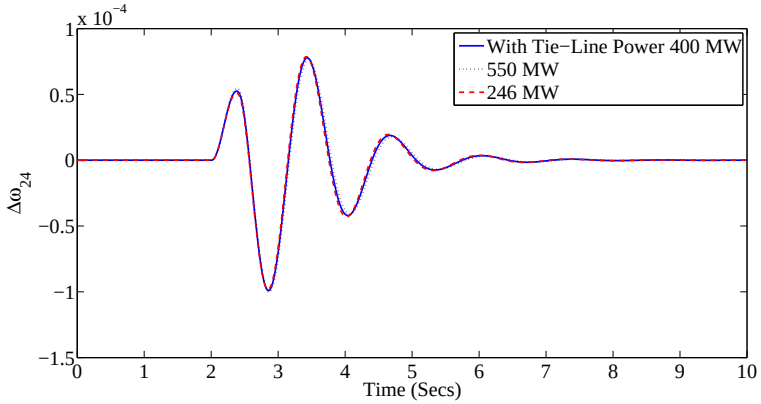

Figure 4.12: $\Delta\omega_{12}$ plot a) without WDC b) With WDC

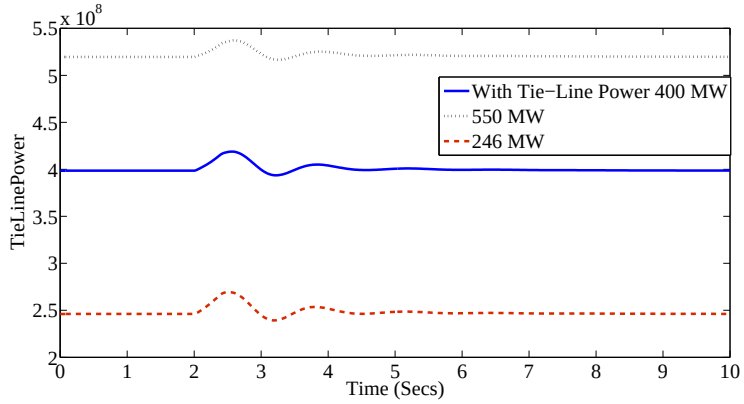

Figure 4.13: Tie-line Power plot a) without WDC b) With WDC

4.1.7 Effect of Delay

To study the effect of delay, the system is simulated considering multiple delays in the wide-area loop. Depending upon channel used, time-delay in WAMS can bee range upto order of 100 msec. First considering a delay in synchronized feedback signal, from Fig. 4.14(a) it can be seen that with the increasing delay the damping is getting reduced and with 50 $msec$ system has gone unstable. Now considering the non-synchronized feedback, delay in the remote signal only, system is simulated. The effect of delay for non-sychronous feedback can be seen in Fig.4.15(b). For both the cases delay degrades the performance of the system. Though delay reduces the damping significantly but still it has more delay-margin compared to synchronized-WDC as shown in Fig. 4.15(b). The system is still stable for time-delay of 100 $msec$ but with poor damping. Although, system was stable robustly for different operating conditions, it loses its stability in delay in wide-area loop.

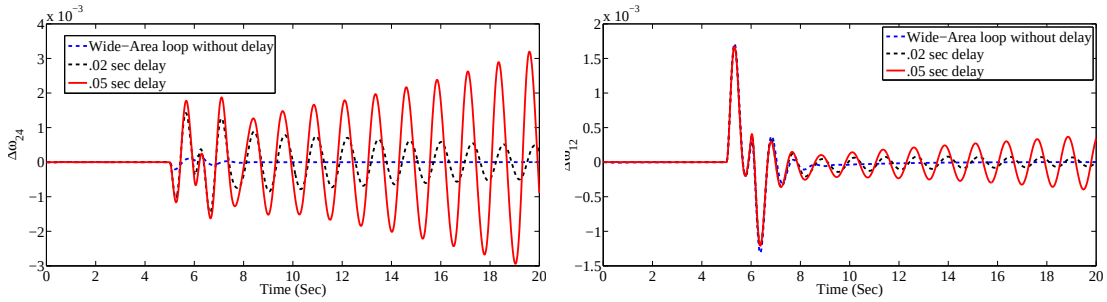

(a) $\Delta\omega_{24}$ plot with time-delays in synchronous feedback

(b) $\Delta\omega_{12}$ plot with time-delays synchronous feedback

Figure 4.14: Responses for variable delays in synchronous feedback

4.1.8 Controller Synthesis (With Considering Delay)

A time delay of 200 ms is considered for the design. To rationalize the system, the time-delay is modeled with 2^{nd} order Pade approximation. The controller is synthesized with the objective of H_∞ with regional pole placement objective. With this much time-delay, the previous controller was counter effective. To study the responses a 0.2 Sec pulse disturbance of a magnitude of $0.05pu$ is given as change in voltage reference at G_2 terminal. Here,

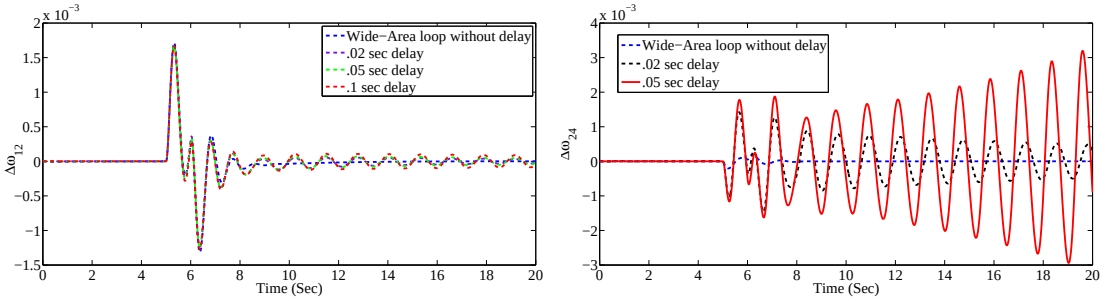

(a) $\Delta\omega_{12}$ plot with time-delays in non-synchronous feedback

(b) $\Delta\omega_{24}$ plot with time-delays in non-synchronous feedback

Figure 4.15: Responses for variable delays in synchronous feedback

considered delay in design is $T_d = 100\ msec$, which is approximated as

$$G_d = \frac{1 - \frac{T_d}{2} + \frac{T_d^2}{4}}{1 + \frac{T_d}{2} + \frac{T_d^2}{4}}$$

.

Synchronous WDC

First considering synchronous feedback configuration, where an equal amount of delays are introduced in both local and remote signals. The block diagram for synchronous WDC is shown in Fig. 4.1.8. Due to time delay equal amount of phase delay has been induced in both the signals. Response to the disturbance is shown in Fig. 4.18. It can be seen that oscillations are being died out within 10 *sec*.

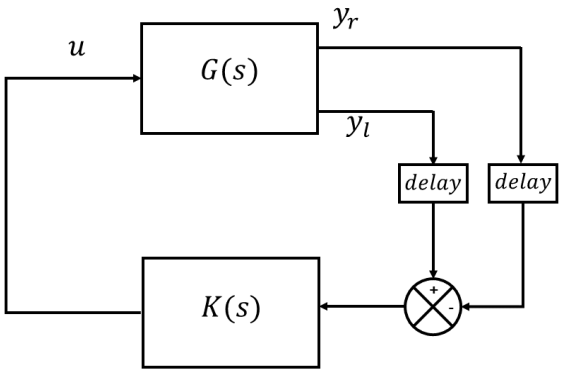

Figure 4.16: Control configuration for Synchronous WDC($K(s)$)

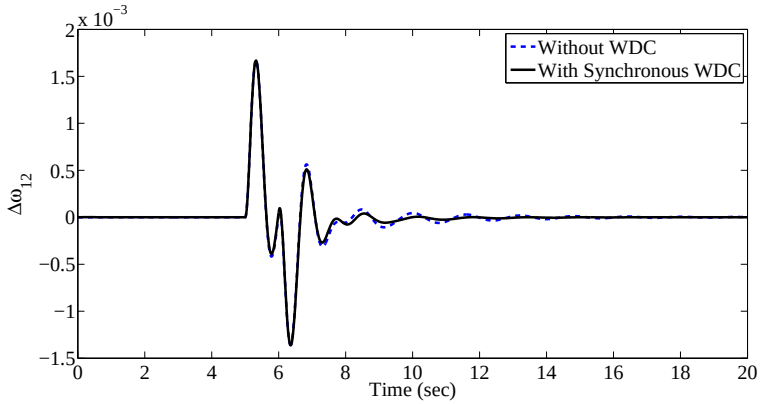

Figure 4.17: $\Delta\omega_{12}$ plot with Synchronous-WDC

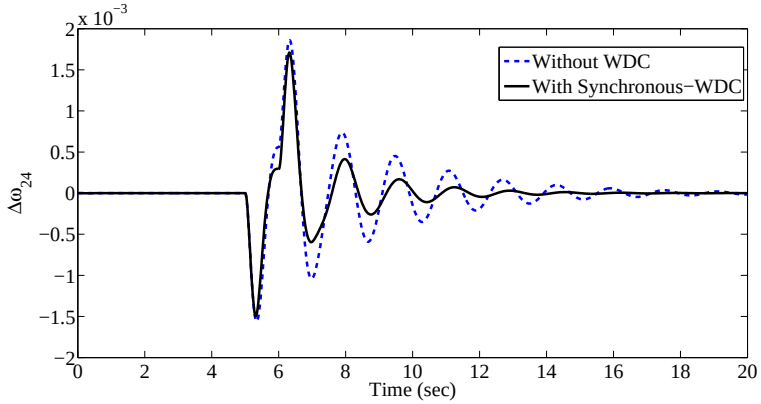

Figure 4.18: $\Delta\omega_{24}$ plot with Synchronous-WDC

Non-Synchronous WDC

Next, in non-synchronized configuration delay is considered in the remote signal only. A functional block diagram for non-synchronous WDC is shown in Fig.4.1.8. The response

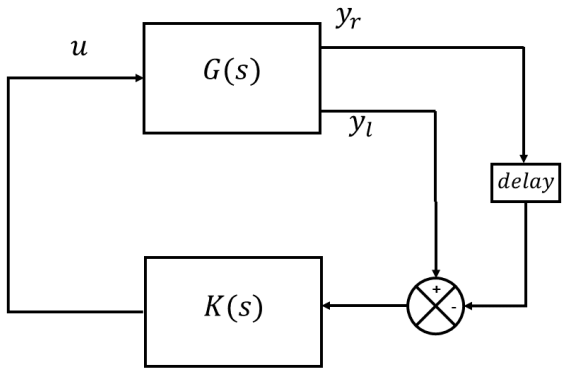

Figure 4.19: Control configuration for Non-Synchronous WDC $K(s)$

of speed deviation to the disturbance is shown in Figs. 4.20,4.21. Though for feedback signal is not synchronized but for performance measure non-delayed synchronized speed deviation is considered. The oscillations due slower mode i.e. inter-area mode is died out very quickly within 4 cycles of operations, which is very impressive. The effect of WDC to the local mode of area 1 can be seen in Fig. 4.20. The WDC marginally improves the damping of it. From small signal analysis, it is found out that the damping of inter-area mode has improved from 0.08 to .255 with the WDC.

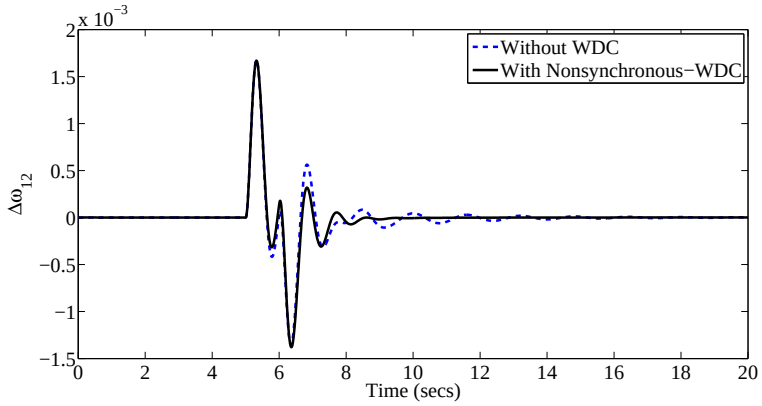

Figure 4.20: $\Delta\omega_{12}$ plot with Non-Synchronous WDC

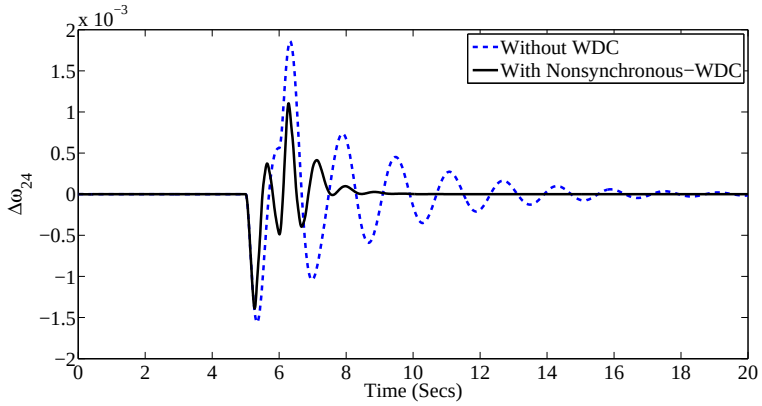

Figure 4.21: $\Delta\omega_{24}$ plot with Non-Synchronous WDC

4.1.9 Evaluation of the performances

System performances with variable delays are considered here for both the synchronous and non-synchronous case. The controllers were designed considering 200ms time delay, so one above i.e.500ms and one below i.e. 50ms delay are considered to evaluate the performance.

Though system stability is robust w.r.t. time delay variation but the performances degrade. For synchronous case, inter-area oscillation has been died out within 10 secs for all delays as shown in Fig.4.22(b). Although the time-delays have a negligible effect on local mode of area 1 but have a significant effect on the local mode of area 2 as shown in 4.22(a) where thw WDC is placed. With different delays it is shown the settling time of local mode has increased. Though delay variations have small impact to inter-area mode but significantly effect the local modes in case of synchronous feedback.

For Non-Synchronous case, the delays in the remote signal are taken as same as the synchronous feedback case. The system performance is well accepted for 500 ms delay although the controller is designed for 200 ms delay as shown in Fig.4.23(b). However, system performance is getting improved if the delay is less than 200 ms, which is reverse in case of the synchronous controller. The variation of delays has no significant effect in local mode also as shown in Fig. 4.23(a), instead in system performs better when delay is less than the assumed value.

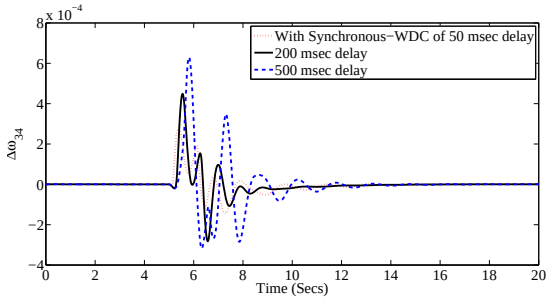

(a) $\Delta\omega_{34}$ plot with Synchronous-WDC for variable delays

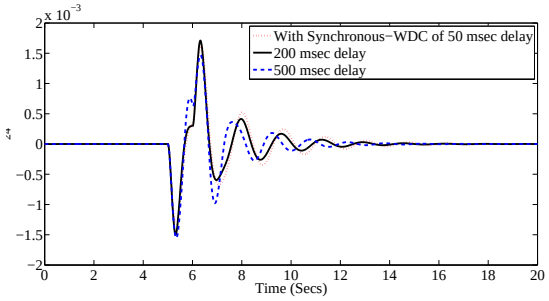

(b) $\Delta\omega_{24}$ plot with Synchronous-WDC for variable delays

Figure 4.22: Responses for variable delays in synchronous feedback

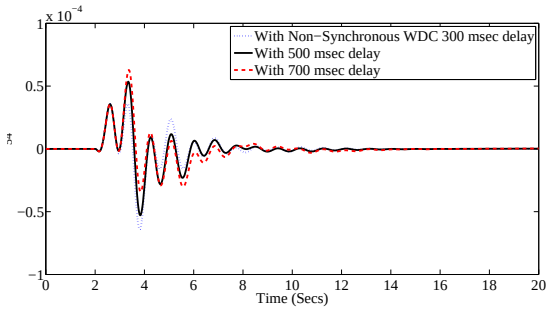

(a) $\Delta\omega_{34}$ plot with Non-Synchronous WDC for different delays

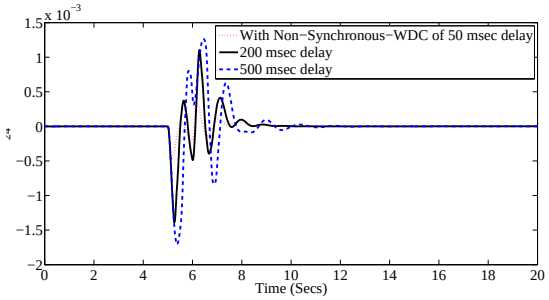

(b) $\Delta\omega_{24}$ plot with Non-Synchronous-WDC for different delays

Figure 4.23: Responses for variable delays in non-synchronous feedback

4.2 Ten Machine Thirty-Nine Bus System

4.2.1 System Description

The above design objective is further implemented in another larger system shown i.e. a 10 machine system 39 bus system [36] also knows as New England Power Grid. The system is of 10 machines and 39 buses, where G_1 to G_9 are equipped with static excitation and local PSSs. G_{10} is a equivalent unit for the study. The system data is taken from [21]. The generation system is modelled as 6^{th} order, exciter as 1^{st} order and LPSS is of 3^{nd} order.

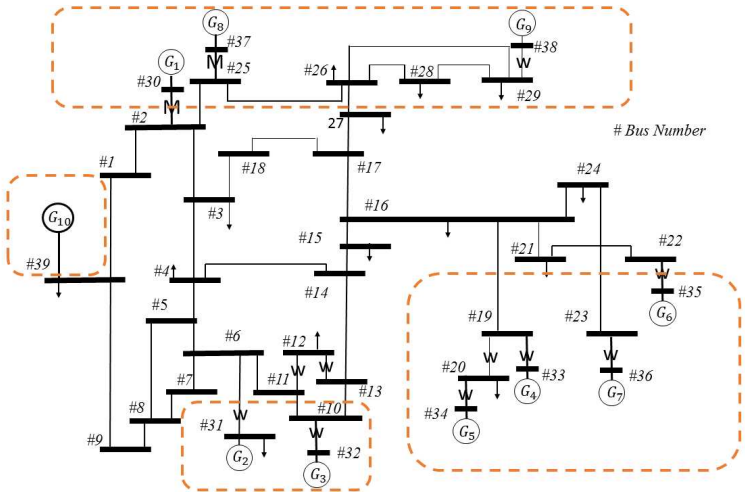

Figure 4.24: Single line diagram for 10 machine system

4.2.2 Modal Analysis

System is modeled in MATLAB-Simulink and linearized it around an operating point. The linearized model came as 96^{th}. From modal analysis it has been found the three inter-area modes are present in the system shown in Table4.3. The mode shapes are shown in Fig.4.25. Here M_2 and M_3 have low damping as M_1 but have relatively larger frequency compared to M_1 so these modes will get settled in less than $10Secs$. Hence designer's prime concern is M_1 i.e. $-0.2768 \pm j3.9179$.

4.2.3 Wide-Area Loop Selection

For wide-area loop selection as in case study I, geometric controllability and observability is measured. As the objective is damping of M_1 mode, so wide-area loop is to be selected

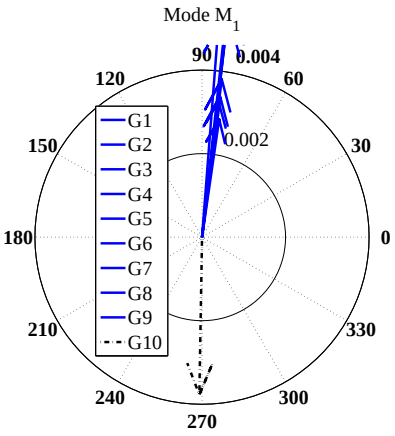

(a) M_1 Mode

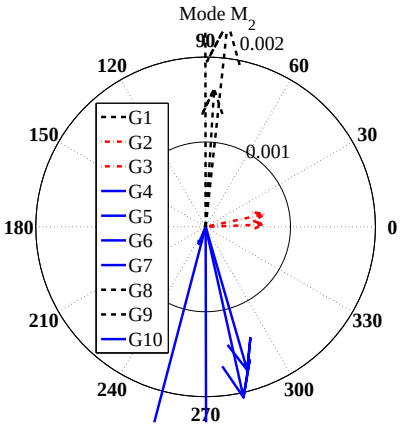

(b) M_2 Mode

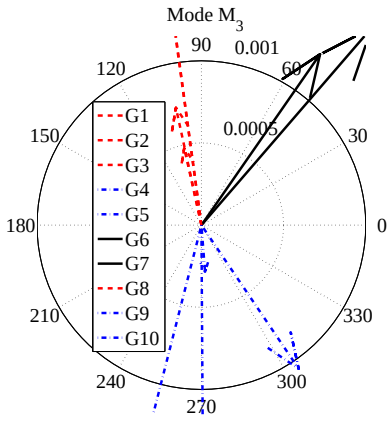

(c) M_3 Mode

Figure 4.25: Mode Shapes of the inter-area modes

Table 4.3: Low frequency modes of the system without WPSS

Mode	Mode Shape	Frequency	Damping
M_1	G_{10} v/s $G_1 - G_9$	0.6236	0.0705
M_2	G_1, G_8, G_9 v/s $G_4 - G_9$	1.04	0.0703
M_3	G_2, G_3 v/s G_4, G_5	0.96	0.0691

which most effective to it and have less coupling to other modes. Here, $\Delta\omega_{10,i}$, where $i = 1, 2.., 9$ are suitable candidates for feedback to the controller. The observability index

for three inter-area modes are shown in Fig.4.27. From Fig 4.27 it can be seen that $\Delta\omega_{10,5}$ gives highest observability index but M_2 M_3 also has high index in the signals. So feedback of this signal may effect the other modes. So next to best is chosen i.e. $\Delta\omega_{10,4}$ which have higher observability of M_1 than the rest and also low observability of other modes. For controller location, controllability index is calculated as shown in Fig.4.26. From Fig.4.26, it can be said that G_4 is suitable location to be equipped with WDC. From analysis G_4 as control input and $\Delta\omega_{10,4}$ is considered as wide-area feedback signal to the controller.

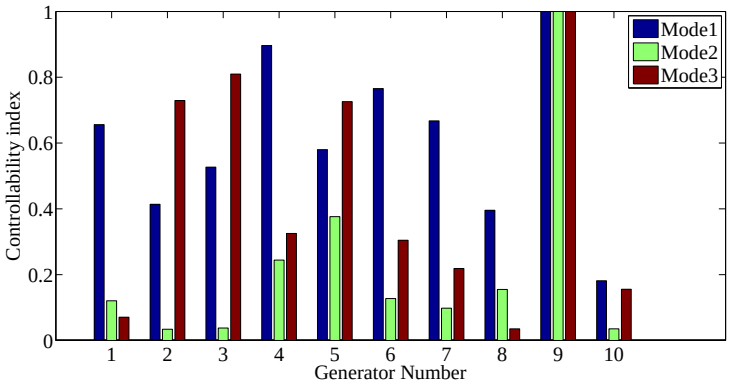

Figure 4.26: Controllability index for 10 machine system

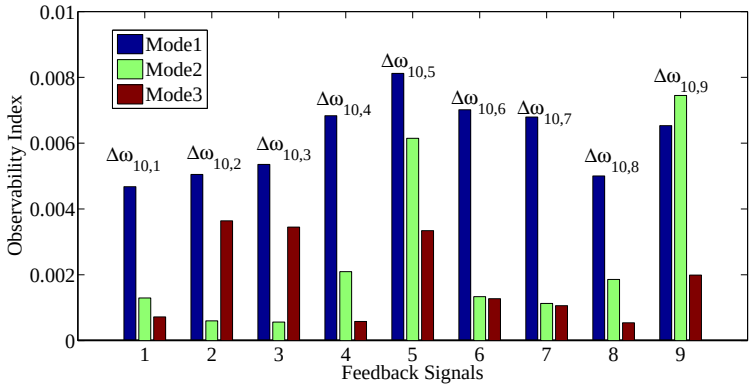

Figure 4.27: Observability index for 10 machine system

4.2.4 Model Order Reduction

The system model was of 96^{th} order which is further reduced to 6^{th} order with *hankel model reduction* method. Reduced order model retain the M_1 mode. The frequency response of original model and reduced order system is shown in Fig.4.28, which shows nearly same

input-output behaviour in desired frequency range.

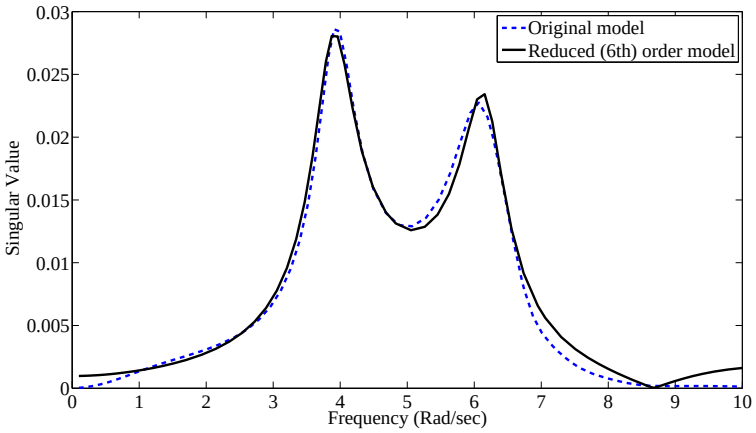

Figure 4.28: frequency response of original system with reduced order model

4.2.5 Controller Synthesis (Without Considering Delay)

The controller is designed considering the reduced order model with H_∞ control with regional pole placement. The weighting function for H_∞ design is considered as $W_1 = \frac{10}{s+10}$,$W_2 = \frac{10s}{s+10}$. To ensure minimum damping of 0.2 a conical region is selected as desired LMI region. Here, to study the effect on local mode of the area where WDC is installed, $\Delta\omega_{5,4}$ i.e. difference between the speed deviation of 5^{th} and 4^{th} machine. Similarly to study the effect of inter-area mode $\Delta\omega_{10,4}$ is considered.

With the WDC, the closed-loop location of the inter-area mode M_1 is found to be $-1.10 \pm j3.91$. From small signal analysis it has been found out that damping of the mode is improved from 0.07 to 0.271. Also, the controller is validated in nonlinear simulation as shown in Fig.4.2.5 and Fig.4.2.5 . A 0.2 sec pulse disturbance of 0.05 magnitude is given at G_4 terminal as a change in voltage reference. As inter-area oscillation is well observed in between the differences of speed deviations G_{10} and G_4, the response for the disturbance is shown in Fig.4.2.5. Where it can be seen that the oscillations died out very quickly compared to without wide-area controller.

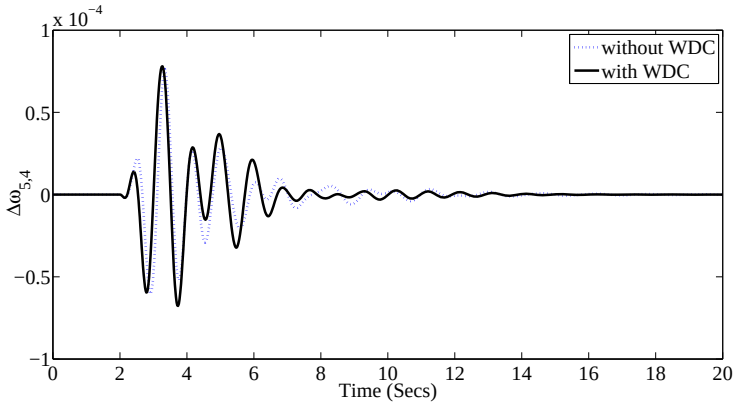

Figure 4.29: $\Delta\omega_{5,4}$ response to the disturbance without WDC and with WDC

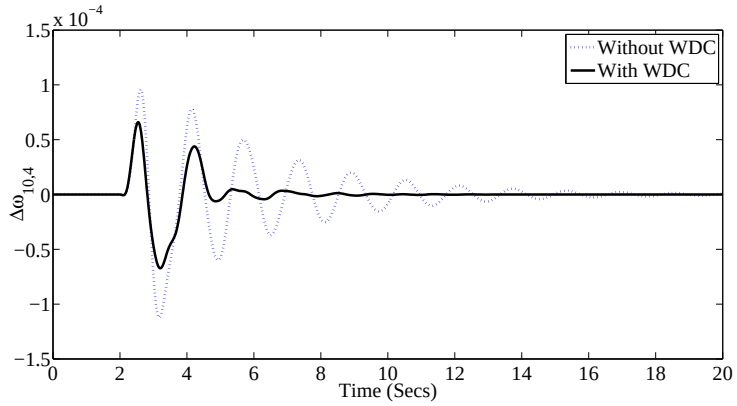

Figure 4.30: $\Delta\omega_{10,4}$ response to the disturbance without WDC and with WDC

4.2.6 Effect of Delays

To study the effect of the delay, a set of delays are considered in the wide-area loop. Same disturbance is given as previous section. First, considering delays in synchronous feedback configuration, the effect can be seen in Fig.(4.2.6) . The system's damping is getting reduced with delays and finally getting unstable with delay greater than 500 $msec$. Similarly, delays are considered in non-synchronous configuration as shown in Fig.(4.2.6). From the Fig. (4.2.6) it can be seen that the non-synchronous configuration has more delay margin but still damping is getting reduced with the increasing delay values. A delay in a system add phase lag and thus makes the control action phase margin less. So, in non-synchronous configuration delay has been observed in local signals, so during analysis it has been observed that local mode of the area go unstable first wrt delay than the inter-area mode.

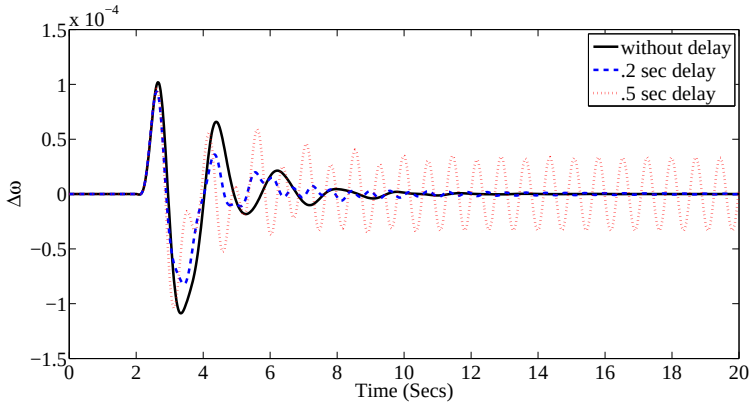

Figure 4.31: $\Delta\omega_{10,4}$ plot for delays in wide-area loop for synchronous feedback

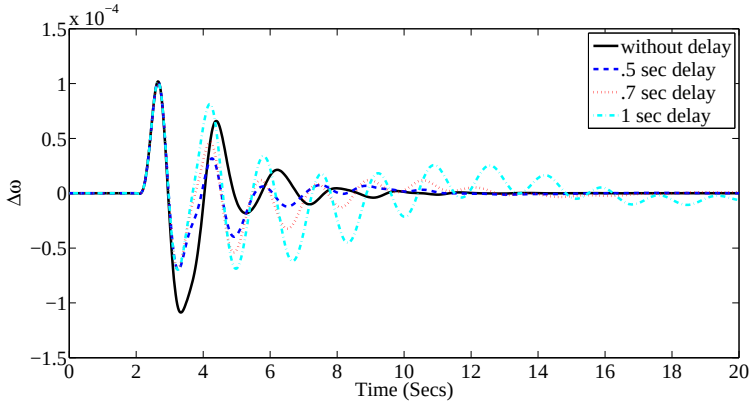

Figure 4.32: $\Delta\omega_{10,4}$ plot for delays in wide-area loop for non-synchronous feedback

4.2.7 Controller Synthesis (With Considering Delay)

A delay near to $500msec$ reduces the performance of the controller significantly. So while synthesis, a delay of $500msec$ is approximated with 2^{nd} order Pade model as

$$G_d = \frac{1 - \frac{T_d}{2} + \frac{T_d^2}{4}}{1 + \frac{T_d}{2} + \frac{T_d^2}{4}}$$

. The controllers are synthesized with the objective of H_∞ sensivity minimization and regional pole placement. Weighting functions and pole placement region are same as of previous design.

Synchronous-WDC

Here, synchronous feedback is considered, where both local and remote signal get synchronized w.r.t. time stamped. Where an equal amount of delays are induced in both local and remote signals. Delay is approximated as 2^{nd} order Pade and the controller is synthesized. From the small signal analysis, the closed-loop inter-area mode is found to be $-.942 \pm j3.87$. Hence, damping is increased from 0.07 to .236. The controller is validated through nonlinear simulation in MATLAB-Simulink where disturbance is added through G_4 as 0.2 sec disturbance at 2 sec after in steady state. The responses are shown in Fig.4.33 and Fig.4.34.

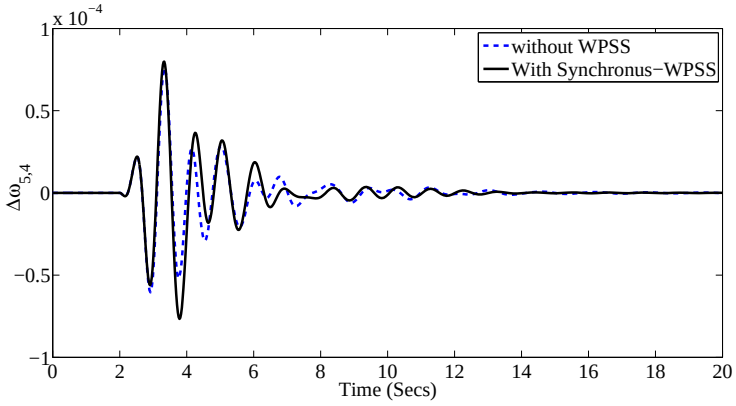

Figure 4.33: $\Delta\omega_{5,4}$ plot with Synchronous WDC

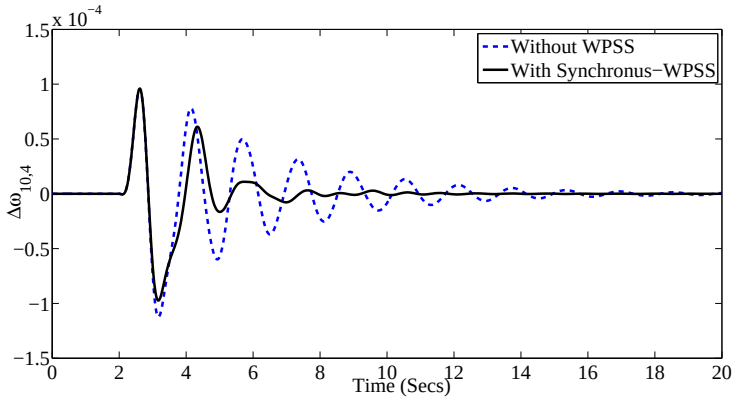

Figure 4.34: $\Delta\omega_{10,4}$ plot with Synchronous WDC

Non-Synchronous WDC

Next, a non-synchronous feedback is considered, no operational delay is considered in signals. Where delay is considered in remote signal only i.e. $\Delta\omega_{10}$. Similar to previous case, a $500msec$ delay is considered which is approximated with Pade 2^{nd} order model and the controller is synthesized. From the linear analysis, the inter-area mode with WDC is found out to be $-1.03 \pm j3.64$. So the damping of inter-area mode is improved from 0.07 to 0.273. The controller is further validated in nonlinear simulation. A $0.2sec$ pulse of the magnitude of 0.05 is given as change in voltage reference at G_4 machine. The response to the disturbance is shown in Figs.4.35,4.36.

In both the cases, inter-area oscillations getting settled quickly less than $5secs$. As extra control modes are added, system responses shows aperiodic behavior. As control modes are well damped, so no counter measures are needed. It can been seen that non-synchronous feedback performs better compared to synchronous feedback. This is probably due to non-delayed feedback signals control action to the inter-area mode. But effect of non-delayed feedback is more visible in local mode. Non-synchronous feedback improves the damping of the local mode too. Whereas no such effect has been observed in synchronous feedback.

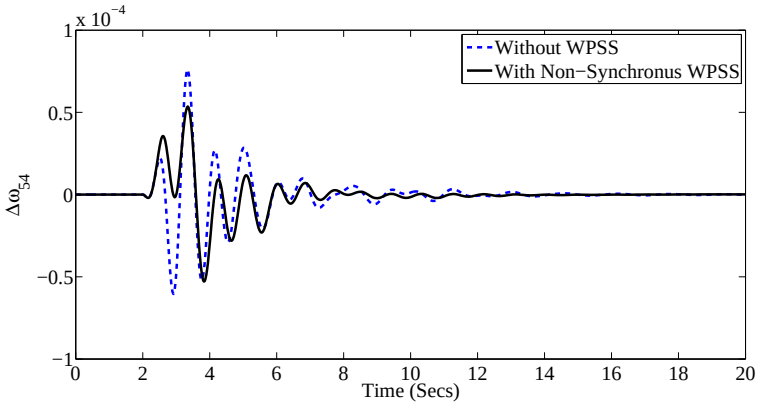

Figure 4.35: $\Delta\omega_{5,4}$ plot with Non-Synchronous WDC

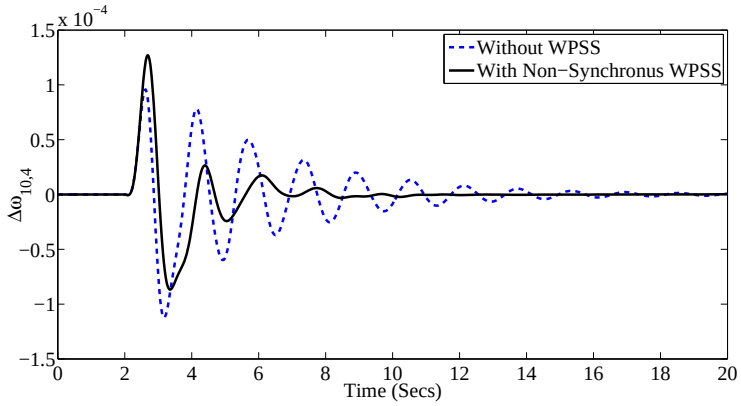

Figure 4.36: $\Delta\omega_{10,4}$ plot with Non-Synchronous WDC

4.2.8 Evaluation of the Performances

System performances with variable delays is considered here for both the synchronous and non-synchronous case. The controllers were designed considering 500 ms time delay, so one above i.e.300ms and one below i.e. 700 ms delay are considered to evaluate the performance. Responses of difference between speed deviations are shown in Figs.(4.37(a),4.37(b),4.38(b),4.38(a)). Though for both the cases closed loop system is stable but performance degrades.

In case of synchronous feedback, change in delays degrade the system performances even though for less delay than designed for. For the delay less than considered delay, settling time has increased but it stays less than 10$secs$ and for the delay larger than 500$msec$ a faster mode of low magnitude has been observed in local speed deviations. The same effect has been observed in inter-area oscillations also. For non-synchronous case, no such effect has been observed. For delay, less than 500$msec$ system performs better than considered delay. For both local and inter-area oscillations system settling time is less than 10$secs$ as shown in Fig.(4.38(a),4.38(b)). In synchronous configuration, delay in wide-area loop have some counter-effect to local mode of the area where WDC is installed, whereas no such deteriorating effect has been observed in non-synchronous configuration as the delay is not present in local signals.

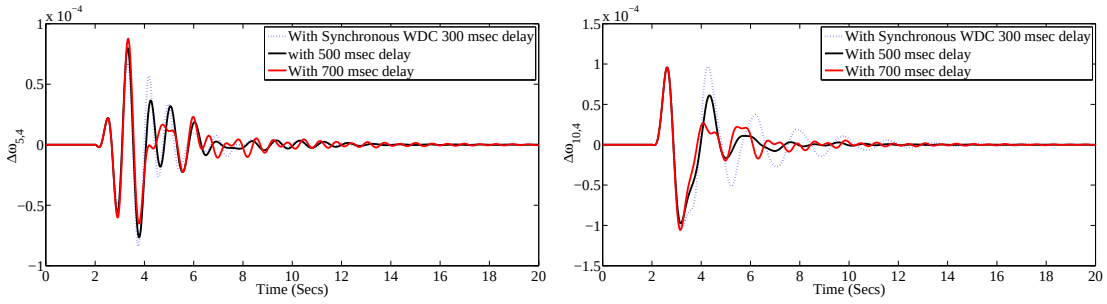

(a) $\Delta\omega_{54}$ plot with Synchronous-WDC for variable delays

(b) $\Delta\omega_{10,4}$ plot with Synchronous-WDC for variable delays

Figure 4.37: Responses for variable delays in synchronous feedback

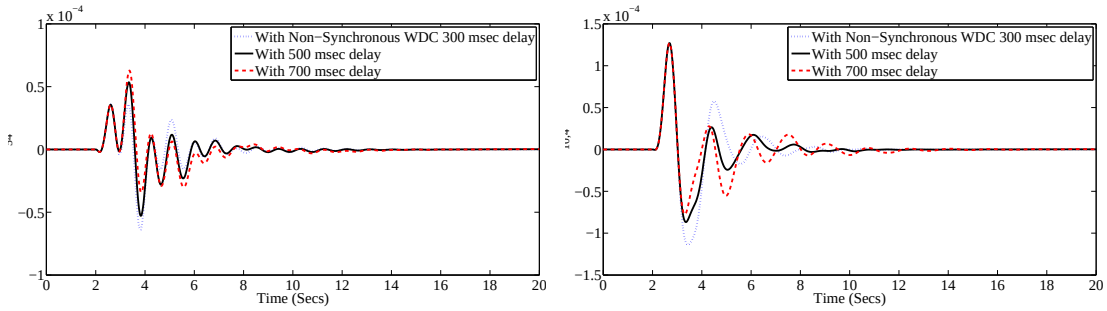

(a) $\Delta\omega_{54}$ plot with Non-Synchronous WDC for variable delays

(b) $\Delta\omega_{10,4}$ plot with Non-Synchronous-WDC for variable delays

Figure 4.38: Responses for variable delays in non-synchronous feedback

CHAPTER 5

Conclusion and Future Scope

5.1 Conclusion

In this thesis, the controller is designed for improving the dynamics of power system in terms of damping of inter-area mode. Two case studies are taken to illustrate the concept. The system is modeled in MATLAB and modal analysis is performed for small signal stability study. It has been observed that inter-area mode were poorly damped with local PSS, due to lack of observability. For efficient control action, wide-area signal loop is selected based upon geometrical measures, also which ensure less effect to other modes. The obtained system mathematical model is of large order, which would increased the computation time. To avoid such problem, model order is reduced by Hankel norm method. With the reduced order model order, the controller is synthesized. At first no-delay has been considered in the design. The controller seems robust against different operating points and disturbances. However, it loses stability for time-delay in wide-area loop. Which illustrated that time-delay should be considered during design stage. Also, it has been observed that delay in non-synchronous configuration have better delay tolerability than synchronous feedback. The time-delay is modeled as 2^{nd} order Pade and it has been shown that it gives a good handle for delay. In synchronous WDC, delay effects the local mode from the area where WDC is located significantly, but as non-synchronous WDC doesnot contain delay in local signal, delay doesnt have any effect on local mode. It has been shown that a Non-Synchronous

WDC works better than Synchronous-WDC. With the change in delay, with synchronous WDC, it degrades the performance with the change in delay. In non-synchronous WDC, no such effect has been observed, also it improves the local mode oscillations.

5.2 Future Scope

Although the present work achieved significant results in study of wide-area controller design and effect of delays in power systems but the work doesn't end here. One can considered the penetration of renewable energy resources in the system and work further with FACTS devices. Also, there is a dedicated area of "networked control system" which can be fused with wide-area control of power system. Also, different control strategy can be applied and a comparison can be done. The present controller design is based upon linear model, one can work on nonlinear model for better performance.

References

[1] "Report on the grid disturbance on 30th july 2012 and 31st july 2012." [Online]. Available: www.cercind.gov.in/2012/orders/Final_Report_Grid_Disturbance.pdf

[2] M. E. Aboul-Ela, A. A. Sallam, J. D. Mccalley, and A. A. Fouad, "Damping controller design for power system oscillations using global signals," *IEEE Trans. Power Syst.,*, vol. 11, May 1996.

[3] G. Andersson, P. Donalek, R. Farmer, N. Hatziargyriou, I. Kamwa, P. Kundur, N. Martins, J. Paserba, P. Pourbeik, J. Sanchez-Gasca *et al.*, "Causes of the 2003 major grid blackouts in north america and europe, and recommended means to improve system dynamic performance," *Power Systems, IEEE Transactions on*, vol. 20, no. 4, pp. 1922–1928, 2005.

[4] J. Arif, N. Chaudhuri, S. Ray, and B. Chaudhuri, "Self-tuning feedback linearization controller for power oscillation damping," in *Transmission and Distribution Conference and Exposition, 2010 IEEE PES*, April 2010, pp. 1–8.

[5] J. Arif, S. Ray, and B. Chaudhuri, "Multivariable self-tuning feedback linearization controller for power oscillation damping," *Control Systems Technology, IEEE Transactions on*, vol. 22, no. 4, pp. 1519–1526, July 2014.

[6] A. Chakrabortty, "Wide-area damping control of large power systems using a model reference approach," in *Decision and Control and European Control Conference (CDC-ECC), 2011 50th IEEE Conference on*, Dec 2011, pp. 2189–2194.

[7] B. Chaudhuri, R. Majumder, and B. Pal, "Application of multiple-model adaptive control strategy for robust damping of interarea oscillations in power system," *Control Systems Technology, IEEE Transactions on*, vol. 12, no. 5, pp. 727–736, Sept 2004.

[8] ——, "Wide-area measurement-based stabilizing control of power system considering signal transmission delay," *Power Systems, IEEE Transactions on*, vol. 19, no. 4, pp. 1971–1979, Nov 2004.

[9] H. Chen, Z. Guo, and H. Bai, "Wide-area robust control with pole placement for damping inter-area oscillations," in *Power Engineering Society General Meeting, 2006. IEEE*, 2006, pp. 7 pp.–.

[10] L. Cheng, G. Chen, W. Gao, F. Zhang, and G. Li, "Adaptive time delay compensator (atdc) design for wide-area power system stabilizer," *Smart Grid, IEEE Transactions on*, vol. 5, no. 6, pp. 2957–2966, Nov 2014.

[11] M. Chenine, K. Zhu, and L. Nordstrom, "Survey on priorities and communication requirements for pmu-based applications in the nordic region," in *PowerTech, 2009 IEEE Bucharest*, June 2009, pp. 1–8.

[12] M. Chilali and P. Gahinet, "$H\infty$ design with pole placement constraints: an LMI approach," *Automatic Control, IEEE Transactions on*, vol. 41, no. 3, pp. 358–367, Mar 1996.

[13] M. Chilali, P. Gahinet, and P. Apkarian, "Robust pole placement in LMI regions," *Automatic Control, IEEE Transactions on*, vol. 44, no. 12, pp. 2257–2270, Dec 1999.

[14] J. Chow, J. J. Sanchez-Gasca, H. Ren, and S. Wang, "Power system damping controller design-using multiple input signals," *Control Systems, IEEE*, vol. 20, no. 4, pp. 82–90, Aug 2000.

[15] A. Domahidi, B. Chaudhuri, P. Korba, R. Majumder, and T. Green, "Self-tuning flexible ac transmission system controllers for power oscillation damping: a case study in real time," *Generation, Transmission Distribution, IET*, vol. 3, no. 12, pp. 1079–1089, December 2009.

[16] S. Ghosh, K. Folly, and A. Patel, "Inter-area oscillating damping with non-synchronous wide-area power system stabilizer, Part-I: Analysis," *Submitted in IEEE Transactions on Power Systems*.

[17] A. Hamdan and A. Elabdalla, "Geometric measures of modal controllability and observability of power system models," *Electric Power Systems Research*, vol. 15, no. 2, pp. 147 – 155, 1988.

[18] A. A. Hashmani and I. Erlich, "Delayed-input power system stabilizer using supplementary remote signals," *Control Engineering Practice*, vol. 19, no. 8, pp. 893 – 899, 2011.

[19] L. H. Hassan, M. Moghavvemi, H. A. Almurib, K. Muttaqi, and H. Du, "Damping of low-frequency oscillations and improving power system stability via auto-tuned {PI} stabilizer using takagisugeno fuzzy logic," *International Journal of Electrical Power and Energy Systems*, vol. 38, no. 1, pp. 72 – 83, 2012.

[20] S. S. Ian Postlethwaite, *Multivariable Feedback Control : Analysis and Design*. Wiley India Pvt Ltd, 2014.

[21] R. Jabr, B. Pal, N. Martins, and J. Ferraz, "Robust and coordinated tuning of power system stabiliser gains using sequential linear programming," *Generation, Transmission Distribution, IET*, vol. 4, no. 8, pp. 893–904, August 2010.

[22] I. Kamwa and L. Gerin-Lajoie, "State-space system identification-toward mimo models for modal analysis and optimization of bulk power systems," *Power Systems, IEEE Transactions on*, vol. 15, no. 1, pp. 326–335, Feb 2000.

[23] I. Kamwa, R. Grondin, and Y. Hebert, "Wide-area measurement based stabilizing control of large power systems-a decentralized/hierarchical approach," *Power Systems, IEEE Transactions on*, vol. 16, no. 1, pp. 136–153, Feb 2001.

[24] I. Kamwa, A. Heniche, G. Trudel, M. Dobrescu, R. Grondin, and D. Lefebvre, "Assessing the technical value of facts-based wide-area damping control loops," in *Power Engineering Society General Meeting, 2005. IEEE*, June 2005, pp. 1734–1743 Vol. 2.

[25] P. V. Kokotovic, R. O'malley, and P. Sannuti, "Singular perturbations and order reduction in control theoryan overview," *Automatica*, vol. 12, no. 2, pp. 123–132, 1976.

[26] P. Korba, M. Larsson, B. Chaudhuri, B. Pal, R. Majumder, R. Sadikovic, and G. Andersson, "Towards real-time implementation of adaptive damping controllers for facts devices," in *Power Engineering Society General Meeting, 2007. IEEE*, June 2007, pp. 1–6.

[27] P. Kundur, I. C. J. T. F. on Stability Terms, and Definitions, "Definition and classification of power system stability." International Conference on Large High Voltage Electric Systems, 2003.

[28] R. Majumder, B. Chaudhuri, H. El-Zobaidi, B. Pal, and I. Jaimoukha, "LMI approach to normalised H_∞ loop-shaping design of power system damping controllers," *Generation, Transmission and Distribution, IEE Proceedings-*, vol. 152, no. 6, pp. 952–960, Nov 2005.

[29] R. Majumder, B. Chaudhuri, B. Pal, and Q.-C. Zhong, "A unified smith predictor approach for power system damping control design using remote signals," *Control Systems Technology, IEEE Transactions on*, vol. 13, no. 6, pp. 1063–1068, Nov 2005.

[30] N. Martins, A. Barbosa, J. Ferraz, M. Dos Santos, A. Bergamo, C. Yung, V. Oliveira, and N. Macedo, "Retuning stabilizers for the north-south brazilian interconnection," in *Panel session on system reliability as affected by power system stabilizers, 1999 IEEE PES Summer Meeting, Edmonton, Canada*, 1999.

[31] F. Milano and M. Anghel, "Impact of time delays on power system stability," *Circuits and Systems I: Regular Papers, IEEE Transactions on*, vol. 59, no. 4, pp. 889–900, April 2012.

[32] N. Mithulananthan, R. Shah, and K. Lee, "Small-disturbance angle stability control with high penetration of renewable generations," *Power Systems, IEEE Transactions on*, vol. 29, no. 3, pp. 1463–1472, May 2014.

[33] M. Mokhtari, F. Aminifar, D. Nazarpour, and S. Golshannavaz, "Wide-area power oscillation damping with a fuzzy controller compensating the continuous communication delays," *Power Systems, IEEE Transactions on*, vol. 28, no. 2, pp. 1997–2005, May 2013.

[34] B. Naduvathuparambil, M. Valenti, and A. Feliachi, "Communication delays in wide area measurement systems," in *System Theory, 2002. Proceedings of the Thirty-Fourth Southeastern Symposium on*, 2002, pp. 118–122.

[35] D. Novosel, M. M. Begovic, and V. Madani, "Shedding light on blackouts," *Power and Energy Magazine, IEEE*, vol. 2, no. 1, pp. 32–43, 2004.

[36] M. Pai, *Energy function analysis for power system stability.* Springer Science & Business Media, 1989.

[37] A. Phadke and R. de Moraes, "The wide world of wide-area measurement," *Power and Energy Magazine, IEEE*, vol. 6, no. 5, pp. 52–65, September 2008.

[38] P.Kundur, *Power System Stability and Control.* McGraw Hill Education (India) Private Limited, 2006.

[39] "Synchrophasors initiatives in india," Anual Technical Report, POSCO, Dec 2013. [Online]. Available: http://posoco.in

[40] C. Scherer, P. Gahinet, and M. Chilali, "Multiobjective output-feedback control via LMI optimization," *Automatic Control, IEEE Transactions on*, vol. 42, no. 7, pp. 896–911, Jul 1997.

[41] D. Soudbakhsh, A. Chakrabortty, and A. Annaswamy, "Delay-aware co-designs for wide-area control of power grids," in *Decision and Control (CDC), 2014 IEEE 53rd Annual Conference on*, Dec 2014, pp. 2493–2498.

[42] H. Tamura, *Large-scale systems control and decision making.* CRC Press, 1990, vol. 64.

[43] C. Taylor, D. C. Erickson, K. Martin, R. Wilson, and V. Venkatasubramanian, "Wacs-wide-area stability and voltage control system: R d and online demonstration," *Proceedings of the IEEE*, vol. 93, no. 5, pp. 892–906, May 2005.

[44] W. Winter, R. Witzmann, G. P. D. Siemens, M. Houry, T. Margotin, F. EDF, J. Zerenyi, M. Rt, H. J. Dudzik, P. SA *et al.*, "Analysis and damping of inter-area oscillations in the ucte/centrel power system."

[45] H. Wu, K. Tsakalis, and G. Heydt, "Evaluation of time delay effects to wide-area power system stabilizer design," *Power Systems, IEEE Transactions on*, vol. 19, no. 4, pp. 1935–1941, Nov 2004.

[46] M. Wu, Y. He, J.-H. She, and G.-P. Liu, "Delay-dependent criteria for robust stability of time-varying delay systems," *Automatica*, vol. 40, no. 8, pp. 1435 – 1439, 2004.

[47] X. Xie, J. Xiao, C. Lu, and Y. Han, "Wide-area stability control for damping interarea oscillations of interconnected power systems," *Generation, Transmission and Distribution, IEE Proceedings*, vol. 153, no. 5, pp. 507–514, September 2006.

[48] W. Yao, L. Jiang, J. Wen, S. Cheng, and Q. Wu, "An adaptive wide-area damping controller based on generalized predictive control and model identification," in *Power Energy Society General Meeting, 2009. PES '09. IEEE*, July 2009, pp. 1–7.

[49] W. Yao, L. Jiang, Q. Wu, J. Wen, and S. Cheng, "Delay-dependent stability analysis of the power system with a wide-area damping controller embedded," *Power Systems, IEEE Transactions on*, vol. 26, no. 1, pp. 233–240, Feb 2011.

[50] W. Yao, L. Jiang, J. Wen, Q. Wu, and S. Cheng, "Wide-area damping controller of facts devices for inter-area oscillations considering communication time delays," *Power Systems, IEEE Transactions on*, vol. 29, no. 1, pp. 318–329, Jan 2014.

[51] ——, "Wide-area damping controller for power system interarea oscillations: A networked predictive control approach," *Control Systems Technology, IEEE Transactions on*, vol. 23, no. 1, pp. 27–36, Jan 2015.

[52] F. Zhang, Y. Sun, L. Cheng, X. Li, J. Chow, and W. Zhao, "Measurement and modeling of delays in wide-area closed-loop control systems," *Power Systems, IEEE Transactions on*, vol. PP, no. 99, pp. 1–8, 2014.

[53] J. Zhang, C. Chung, C. Lu, K. Men, and L. Tu, "A novel adaptive wide area pss based on output-only modal analysis," *Power Systems, IEEE Transactions on*, vol. PP, no. 99, pp. 1–10, 2014.

[54] J. Zhang, C. Chung, and Y. Han, "A novel modal decomposition control and its application to pss design for damping interarea oscillations in power systems," *Power Systems, IEEE Transactions on*, vol. 27, no. 4, pp. 2015–2025, Nov 2012.

[55] J. Zhang, C. Chung, S. Zhang, and Y. Han, "Practical wide area damping controller design based on ambient signal analysis," *Power Systems, IEEE Transactions on*, vol. 28, no. 2, pp. 1687–1696, May 2013.

[56] Y. Zhang and A. Bose, "Design of wide-area damping controllers for interarea oscillations," *Power Systems, IEEE Transactions on*, vol. 23, no. 3, pp. 1136–1143, Aug 2008.

[57] A. Zolotas, B. Chaudhuri, I. Jaimoukha, and P. Korba, "A study on lqg/ltr control for damping inter-area oscillations in power systems," *Control Systems Technology, IEEE Transactions on*, vol. 15, no. 1, pp. 151–160, Jan 2007.